SCF β TrCP mediates stress-activated MAPK-induced Cdc25B degradation

$SCF^{\beta TrCP}$ mediates stress-activated MAP kinase-induced Cdc25B degradation

Sanae Uchida[1], Nobumoto Watanabe[2], Yasusei Kudo[3], Katsuji Yoshioka[4], Tsukasa Matsunaga[5], Yukihito Ishizaka[6], Hitoshi Nakagama[7], Randy Y.C. Poon[8], and Katsumi Yamashita[5,]

[1]Venture Business Laboratory, Center for Innovation, [4]Division of Molecular Cell Signaling, Cancer Research Institute, and [5]Division of Pharmaceutical Sciences, Institute of Medical, Pharmaceutical and Health Sciences, Kanazawa University, Kakuma, Kanazawa 920-1192, Ishikawa, Japan

[2]Chemical Library Validation Team, Chemical Biology Core Facility, Chemical Biology Department, RIKEN ASI, Wako 351-0198, Saitama, Japan

[3]Department of Oral Maxillofacial Pathobiology, Division of Frontier Medical Science, Graduate School of Medical Sciences, Hiroshima University, Hiroshima 734-8553, Japan

[6]Division of Intractable Diseases, Research Institute, National Center for Global Health and Medicine, Tokyo 162-8655, Japan

[7]Early Oncogenesis Research Project, National Cancer Center Research Institute, Tokyo 104-0045, Japan

[8]Division of Life Science, The Hong Kong University of Science and Technology, Clear Water Bay, Hong Kong

Corresponding author: Katsumi Yamashita, PhD: Division of Pharmaceutical Sciences, Institute of Medical, Pharmaceutical and Health Sciences, Kanazawa University, Kakuma, Kanazawa 920-1192, Ishikawa, Japan.

Tel: +81 76 264 6270, Fax: +81 76 264 6270, E-mail: katsumi@kenroku.kanazawa-u.ac.jp

Running title: Cdc25B ubiquitylation by $SCF^{\beta TrCP}$

Keywords: Cdc25B, $SCF^{\beta TrCP}$, phosphorylation, PEST-like

Summary

Of the three mammalian CDK-activating Cdc25 protein phosphatases (Cdc25A, B, and C), Cdc25A protein is degraded via $SCF^{\beta TrCP}$-mediated ubiquitylation following genomic insult; however, the regulation of the stability of the other two Cdc25 proteins is not well understood. Previously, we showed that Cdc25B is primarily degraded by cellular stresses that activate stress-activated MAP kinases, such as c-Jun NH_2-terminal kinase (JNK) and p38. Here, we report that Cdc25B was ubiquitylated by $SCF^{\beta TrCP}$ E3 ligase upon phosphorylation at two serine (Ser) residues in the βTrCP-binding motif-like sequence ^{94}DAGLCMDSPSP^{104}. Point mutation of these Ser residues to alanine (Ala) abolished the JNK-induced ubiquitylation by $SCF^{\beta TrCP}$, and point mutation of DAG to AAG or DAA eradicated both βTrCP binding and ubiquitylation. Further analysis of the mode of βTrCP binding to this region revealed that the PEST-like sequence from ^{82}ESS to ^{94}DAG is critically involved in both the βTrCP binding and ubiquitylation of Cdc25B. Furthermore, the phospho-mimetic substitution of all 10 Ser residues from ^{82}ESS to SPSP^{104} to Asp resulted in βTrCP binding. Collectively, these results indicate that stress-induced Cdc25B ubiquitylation by $SCF^{\beta TrCP}$ requires the phosphorylation of ^{101}SP^{103}SP in the βTrCP-binding motif-like and adjacent PEST-like sequences.

Introduction

Cdc25 dual-specificity phosphatases promote cell cycle progression via the activation of cyclin-dependent kinase (CDK) cyclin by removing inhibitory phosphate groups on CDK (Morgan, 1995; Boutros *et al*., 2006). Higher Metazoa possess three isoforms of Cdc25, *i.e*., Cdc25A, B, and C. These are largely considered to serve roles in different cell cycle phases: Cdc25A in the G1/S to S phase, and Cdc25B and C in the G2/M to M phase (Boutros *et al*., 2006). However, this is not strictly correct because the depletion of either one or two *Cdc25* genes does not produce a defective phenotype in the normal cell cycle, indicating that their roles overlap in somatic cell cycle control (Chen *et al*., 2001; Lincoln *et al*., 2002; Ferguson *et al*., 2005; Ray *et al*., 2007; Lee *et al*., 2009).

Of the three mammalian Cdc25 isoforms, Cdc25A has received special attention because it is a target of the DNA replication/damage checkpoint (Donzelli and Draetta, 2003; Bartek *et al*., 2004) and is the only Cdc25 that is essential to mouse embryogenesis (Ray *et al*., 2007; Lee *et al*., 2009). Cdc25A is phosphorylated rapidly by CHK1 upon genomic damage/replication arrest, and this is followed by the phosphorylation of critical serine (Ser) residues in the βTrCP-binding DSG motif by NEK11 (Busino *et al*., 2003; Jin *et al*., 2003; Melixetian *et al*., 2009), which initiates

$SCF^{\beta TrCP}$-mediated ubiquitylation and degradation (Busino *et al*., 2004). Moreover, Cdc25A is directly linked to tumorigenesis, and the frequent overexpression of Cdc25A in human cancers is well documented (Kristjansdottir and Rudolph, 2004; Boutros *et al*., 2007).

The WD repeat-containing F-box protein βTrCP is a substrate-binding component of SCF (Skp1/Cul1/F-box protein) E3 ubiquitin ligase that recognises the doubly phosphorylated conserved motif DSGxxS (S can be replaced by T, and x represents any amino acid; Winston *et al*., 1999; Latres *et al*., 1999). $SCF^{\beta TrCP}$ targets a number of proteins that regulate the cell cycle and apoptosis (Frescas and Pagano, 2008). In particular, some proteins that control the G2/M transition, such as Cdc25A, Emi1, Wee1A, and Bora, are $SCF^{\beta TrCP}$ substrates, and most of them contain the above-mentioned βTrCP-binding sequence (Busino *et al*., 2003; Jin *et al*., 2003; Margottin-Goguet *et al*., 2003; Guardavaccaro *et al*., 2003; Watanabe *et al*., 2004; Seki *et al*., 2008). Wee1 kinase is also a substrate of $SCF^{\beta TrCP}$, but its proposed βTrCP-binding sequence deviates from the consensus sequence (Watanabe *et al*., 2004). The consensus sequence and its deviated phosphopeptides bind βTrCP by forming hydrogen bonds and electrostatic interactions (Wu *et al*., 2003). In addition to such

phosphopeptides, Cdc25A and Cdc25B possess the non-phosphorylated βTrCP-binding sequence DDGxxD (Kanemori *et al*., 2005).

Similar to Cdc25A, Cdc25B can transform pRB-negative cells or normal cells when co-expressed with the oncogenic *ras* (Galaktionov *et al*., 1995). Cdc25B overexpression is also found in human cancers and is correlated with a poor prognosis, as in the case of Cdc25A (Kristjansdottir and Rudolph, 2004; Boutros *et al*., 2007). The tumorigenic activity of Cdc25B is partly explained by an increase in hyperplasia or susceptibility to carcinogens in Cdc25B transgenic mice (Ma *et al*., 1999; Yao *et al*., 1999). Moreover, Cdc25B overexpression accelerates mitotic entry (Karlsson *et al*., 1999) and overrides the radiation-induced G2 checkpoint *in vitro* (Miyata *et al*., 2001).

Recently, we showed that Cdc25B is degraded rapidly by non-genotoxic stimuli that activate stress-responsive MAP kinases, such as c-Jun N-terminal kinase (JNK) and p38 (Uchida *et al*., 2009). Our results suggested that these kinases phosphorylate specific Ser residues in the N-terminal region (S101 and S103) to induce Cdc25B degradation. We also found that HeLa cells expressing the non-phosphorylatable S101A mutant Cdc25B were more refractory to anisomycin-induced G2 arrest than wild-type HeLa cells.

Here, we report that JNK-induced Cdc25B ubiquitylation is mediated by F-box protein βTrCP-containing SCF ubiquitin ligase. We show that S101 and S103 are phosphorylated upon non-genotoxic stress and that βTrCP binds the sequence around S101/103 of Cdc25B in a phosphorylation-dependent manner, even when the DSG consensus βTrCP binding sequence is replaced with DAG. Our data also indicate that full binding and ubiquitylation of Cdc25B by $SCF^{\beta TrCP}$ requires an upstream ESS-rich PEST-like sequence, as well as DAG and S101/S103 phosphorylation.

Results

Ubiquitylation of Cdc25B is carried out by $SCF^{\beta TrCP}$ and is controlled by JNK

Our previous report suggested that non-genotoxic stress-induced Cdc25B degradation was mediated by the ubiquitin-proteasome pathway via S101 and S103 phosphorylation by JNK/p38 (Uchida *et al*., 2009). Fig. 1A shows that the amino acid sequence surrounding Cdc25B S101/103 is quite similar to that in Cdc25A, which is a substrate of $SCF^{\beta TrCP}$ E3 ubiquitin ligase (Busino *et al*., 2003; Jin *et al*., 2003). Despite the overall similarity, the critical βTrCP-binding motif of Cdc25A (DSG) is replaced with DAG in Cdc25B, and DAG is reported to be inactive for βTrCP binding in humans and *Xenopus* Cdc25A (Busino *et al*., 2003; Jin *et al*., 2003; Kanemori *et al*., 2005).

The corresponding region of Cdc25B, including the human splice variants Cdc25B2 and Cdc25B3 and mouse Cdc25B1, has a similar amino acid sequence (Fig. 1A; Baldin *et al*., 1997; Kakizuka *et al*., 1992). As indicated in Fig. 1B, human Cdc25B3, mouse Cdc25B1, and human Cdc25B1 were also degraded on coexpression with JNK or p38 (hereafter, we refer to human Cdc25B1 as Cdc25B). Interestingly, the Cdc25B/D94A mutant was refractory to JNK- or p38-induced degradation, suggesting the involvement of βTrCP binding (Fig. 1B).

Next, we investigated the JNK-dependent interaction between βTrCP1 and Cdc25B. We compared βTrCP binding to the Cdc25B of the wild type and a mutant that lacked the constitutive βTrCP-binding motif by mutating ^{254}DDG to DAA, which hereafter is referred to as Cdc25B^{DAA}. Although wild-type Cdc25B bound βTrCP1 irrespective of the JNK activity, Cdc25B^{DAA} interacted with βTrCP1 in a JNK-dependent manner (Fig. 1C). In wild-type Cdc25B, JNK induced Cdc25B degradation and apparent Cdc25B binding was not as enhanced. Given the JNK-induced Cdc25B degradation that occurred in wild-type Cdc25B, several times more βTrCP was estimated to bind Cdc25B on co-expression with JNK. Likewise, the Cdc25B N-terminal fragment displayed JNK-dependent βTrCP1 binding, whereas the C-terminal fragment with the DDG site showed that βTrCP bound in a JNK-independent manner

(Fig. 1D). Furthermore, Cdc25B^{DAA} interacted with βTrCP1 and βTrCP2, but not with other F-box proteins, such as Skp2 and Cdc4 (Fig. 1E). Cdc25B^{DAA} was stabilised when cotransfected with the F-box deletion mutant βTrCP1$^{\Delta F}$, which lacks ubiquitylation activity due to its inability to bind to the core SCF complex, but retains substrate-binding ability via an intact WD domain (Fig. 1E).

Next, we investigated the ubiquitylation of Cdc25B by SCF$^{\beta TrCP}$ *in vitro*. ^{35}S-labelled Cdc25B^{DAA} was efficiently ubiquitylated by SCF containing βTrCP1 or βTrCP2 in a JNK-dependent manner. In contrast, no ubiquitylated signal was detected when Skp2 or Cdc4 was used as the F-box protein (Fig. 2A). Furthermore, βTrCP1$^{\Delta F}$ did not ubiquitylate Cdc25B (Fig. 2B). Note that SCF$^{\beta TrCP1}$ and SCF$^{\beta TrCP2}$ could ubiquitylate Cdc25B^{DAA} without JNK, but JNK clearly enhanced the ubiquitylation (Fig. 2A and 2B). A high level of ubiquitylation was observed in the absence of JNK when wild-type Cdc25B was used for the *in vitro* ubiquitylation assay (Fig. 2C). Nevertheless, slight enhancement of Cdc25B ubiquitylation by SCF$^{\beta TrCP1}$ was observed in the presence of JNK activity (Fig. 2C). These results indicate that SCF$^{\beta TrCP}$ binds and ubiquitylates Cdc25B in a JNK-dependent manner, which is independent of the DDG constitutive binding site, and that a new JNK-regulated βTrCP-binding site is located in the N-terminal 175 amino acids of Cdc25B.

Our previous report suggested that S101 and S103 were possible target sites of JNK or p38 (Uchida *et al*., 2009). Therefore, we assessed the contributions of S101 and S103 to $SCF^{\beta TrCP}$-mediated $Cdc25B^{DAA}$ ubiquitylation. As indicated in Fig. 2D, whereas the ubiquitylation of Cdc25B was greatly compromised by S101A or S103A mutations, it was almost completely abolished with a S101/103A double mutant. These results indicate that the effects of S101 and S103 on Cdc25B ubiquitylation were collaborative. Other Cdc25B proteins, such as human Cdc25B3 and mouse Cdc25B1, were also ubiquitylated by $SCF^{\beta TrCP1}$ in the presence of JNK1 (Fig. S1A). Intriguingly, $Cdc25B^{D94A}$ was hardly ubiquitylated (Fig. S1A), suggesting that D94 in DAG is involved in JNK-induced Cdc25B ubiquitylation. Moreover, in such wild-type or mutant Cdc25B, βTrCP1binding to Cdc25B proteins were roughly proportional to their ubiquitylation level (Fig. S1B). Collectively, these results clearly indicate that JNK-induced Cdc25B degradation is mediated by $SCF^{\beta TrCP1}$, and that the phosphorylation of Cdc25B S101 and S103 plays an important role in this process.

JNK-induced Cdc25B degradation is aborted by βTrCP depletion

Next, we assessed the effects of βTrCP depletion on JNK-induced Cdc25B degradation using siRNA that targets both βTrCP1 and βTrCP2. We used either one

siRNA used in previous reports (Margottin-Goguet *et al*., 2003; Guardavaccaro *et al*., 2003; denoted here as pan-βTrCP) or two in combination, which enabled us to knockdown either βTrCP1 or βTrCP2 specifically (denoted as βTrCP1 + 2). The effect of βTrCP depletion on introducing these siRNAs to HeLa-W40 cells that stably express FLAG-Cdc25B (Uchida *et al*., 2009) is shown in Fig. S2A (we show only the expression of βTrCP1, due to the lack of a specific antibody to βTrCP2). The results also indicated that the application of such siRNA to HeLa-W40 cells enhanced the expression of FLAG-Cdc25B and endogenous Cdc25A, suggesting that both Cdc25A and Cdc25B are destroyed via a βTrCP-mediated pathway, even in the absence of cellular stress (Fig. S2A).

First, we examined the stability of endogenous Cdc25B after siRNA depletion of βTrCP1 and 2 with either siRNA for pan-βTrCP or combined siRNA for βTrCP1 and 2. As indicated in Fig. 3A, βTrCP depletion endowed dramatic resistance to endogenous Cdc25B under anisomycin stress. Moreover, transiently expressed $Cdc25B^{DAA}$ also became refractory to the JNK-induced degradation on βTrCP1/2 depletion (Fig. S2B). As the depletion of βTrCP1 and 2 with the two siRNA treatments gave similar results (Fig. 3A and S2A), we mainly used pan-βTrCP siRNA in the subsequent experiments.

Next, we asked whether the half-life of Cdc25B was affected by βTrCP depletion. HeLa-W40 cells stably expressing FLAG-Cdc25B were depleted of βTrCP1/2 with pan-βTrCP siRNA and the expression of Cdc25B protein was determined in the presence of cycloheximide. As indicated in Fig. 3B, wild-type Cdc25B appeared to be stabilised in βTrCP-depleted cells. Interestingly, the steady-state expression of constitutively expressed $Cdc25B^{DAA}$ in HeLa-DAA34 cells was also enhanced by βTrCP depletion (Fig. 3C), suggesting that the $SCF^{\beta TrCP}$-mediated ubiquitin–proteasome pathway controls Cdc25B stability in unstressed conditions, through a site other than the DDG βTrCP-binding site.

We further investigated the involvement of βTrCP in anisomycin-induced Cdc25B degradation. FLAG-$Cdc25B^{WT}$-expressing HeLa-W40 cells were transfected with either luciferase or pan-βTrCP siRNA, followed by a 50 ng/mL anisomycin challenge. βTrCP1/2 depletion strongly compromised anisomycin-induced Cdc25B degradation (Fig. 3D). βTrCP depletion of FLAG-$Cdc25B^{DAA}$-expressing HeLa-DAA34 cells had similar effects (Fig. S2B). Collectively, these results unequivocally indicate that $SCF^{\beta TrCP}$ directly controls the non-genotoxic stress-induced instability of Cdc25B. Furthermore, these results also suggest that a site other than the constitutive binding site of DDG controls the steady-state stability of Cdc25B.

JNK phosphorylates Cdc25B under stressful conditions

Next, we investigated whether JNK/p38 phosphorylated S101 and S103 by raising antibodies that recognised S101-, S103-, or S101/103-phosphorylated Cdc25B; the antibody specificity is shown in Fig. S3A. Using these antibodies, we investigated the phosphorylation status of S101 and S103 under either unstressed or stressed conditions. Conventional HeLa cells were not useful in these experiments because we could not recover enough Cdc25B by immunoprecipitation to detect Cdc25B phosphorylation. Then, we used HeLa-W40 cells were used for phosphorylation analyses. Although a slight, but obvious, phospho-S101 signal was detected under unstressed conditions, S101 phosphorylation increased dramatically within 5 min of the 50 ng/mL anisomycin treatment, concomitant with p38 activation judging from the appearance of the phosphorylated form of MK2 (Fig. 4A). Unlike S101, the S103 phosphorylation signal was undetectable at time 0. A slight increase in phosphorylation was detected at 5 min and a much stronger signal was detected at 10 min, at which point JNK was fully activated judging from the phospho-c-Jun signal. The results for phospho-S103 were similar to those for S101/103 double phosphorylation, in which the maximum level was detected at 10 min. Cdc25B phosphorylation decreased at 15 min

and disappeared completely thereafter due to Cdc25B degradation. Similar results were obtained for stress induced with 300 mM NaCl (Fig. 4B) or ultraviolet (UV) irradiation (Fig. S3B). The steady-state phosphorylation of S101 and the similarity in the pattern between phospho-S103 and phospho-S101/103 suggest that the phosphorylation of S103 occurs in S101-phosphorylated Cdc25B, because S101 is always phosphorylated in the absence of stress.

Next, we investigated the effects of p38 inhibitors (*i.e.*, SB202190 and PD169316; abbreviated SB and PD, respectively) or JNK inhibitors (*i.e.*, SP600125 or SP) on Cdc25B phosphorylation in HeLa-W40 cells. First, we determined suitable concentrations of these inhibitors for the specific inhibition of the respective kinases, because these kinases are often cross-inhibited by such inhibitors. As shown in Fig. S4A, 20 μM SB inhibited both p38 and JNK activity judging from the disappearance of the phospho-MK2 and phospho-c-Jun signals, respectively, and it specifically inhibited p38 at a concentration as low as 5 μM without JNK inhibition. Figs. S4B and S4C also indicate that 5 μM PD and 20 μM SP are suitable for the specific inhibition of p38 and JNK, respectively, without obvious cross-inhibition. As indicated in Fig. 4C, anisomycin-induced S101 phosphorylation was reduced by the p38 inhibitors SB and PD, but these inhibitors did not affect S103 phosphorylation. In comparison, the JNK

inhibitor SP completely inhibited S103, and modest inhibition of S101 phosphorylation was also observed. The role of JNK in S103 and S101 phosphorylation was also indicated by the siRNA depletion of JNK1 and JNK2 in anisomycin-treated HeLa-W40 cells, where the phospho-S101 signal was reduced and the phospho-S101/103 signal was almost completely abolished by the knockdown of both JNK1 and 2 (Fig. 4D). In a similar context, the clear reduction of the expression of endogenous Cdc25B by the transfection of wild-type, but not the kinase-dead mutant JNK1, also suggests that JNK functions in the degradation of endogenous Cdc25B (Fig. S4D).

Collectively, these and our previous results indicate that the enhanced phosphorylation at S101 caused by p38 and JNK and *de novo* S103 phosphorylation by JNK play critical roles in stress-induced Cdc25B degradation. Furthermore, the phospho-S101 signal detected under unstressed conditions did not disappear completely with the p38 inhibitors or JNK inhibitor, suggesting that an unidentified kinase(s) that phosphorylates S101 is involved in steady-state Cdc25B degradation.

The βTrCP-binding motif-like DAG is essential for SCF^{βTrCP}-mediated Cdc25B ubiquitylation

The above results suggested that DAG, currently believed to be inactive, is functional in βTrCP-mediated Cdc25B ubiquitylation. To explore this possibility, we made a mutant Cdc25B in which DAG was mutated to AAG (D94A), as the D (Asp) in DSG plays a critical role in substrate binding to βTrCP (Wu *et al*., 2003), and investigated whether the DAG in Cdc25B functions in JNK-induced βTrCP binding. FLAG-Cdc25B^{D94A} was cotransfected with βTrCP1 in the presence or absence of JNK1, and its binding to βTrCP1 was determined. Interestingly, Cdc25B^{D94A} failed to bind βTrCP1 (Fig. 4A). Cdc25B^{G96A} (DAA instead of DAG) was also unable to bind βTrCP1 (Fig. 4A). Furthermore, Fig. S5A shows that both Cdc25B^{D94A} and Cdc25B^{G96A} were refractory to JNK-induced degradation (see also Fig. 1B). As expected, the Cdc25B S101/103A double mutant also lost βTrCP-binding ability. These results suggest that the Cdc25B peptide from ^{94}DAG to ^{101}SPSP is a minimal requirement for βTrCP binding (see Fig. 1A). Moreover, the steady-state expression of such mutant Cdc25B was much higher than that of the wild type (Fig. 5A). Therefore, the DAG sequence seems to be deeply involved in both the steady-state and stress-induced degradation of Cdc25B.

Next, we investigated how mutations in the DAG sequence affected *in vitro* Cdc25B ubiquitylation. Cdc25B^{D94A} was not ubiquitylated by SCF$^{\beta TrCP1}$, even in the presence of JNK activity; its ubiquitylation level was much less than that of the S101/103 double mutant (Fig. 5B). Cdc25B ubiquitylation was also greatly compromised by a G96A mutation, suggesting that G96 plays a role in Cdc25B binding to βTrCP. Cdc25B^{D94A} was phosphorylated at S101/103 when JNK1 was cotransfected (Fig. S5B), showing that the phosphorylation of SPSP occurs irrespective of DAG. These results indicate that DAG in Cdc25B is necessary for ubiquitylation by SCF$^{\beta TrCP}$.

To elucidate whether a peptide encompassing DAG to SPSP was sufficient for βTrCP binding, we analysed βTrCP1 binding based on DAGLCMDSPSP peptides, including the unphosphorylated, phospho-S101, and phospho-S101/103 forms. Peptide-conjugated beads were incubated with crude cell extracts prepared from βTrCP1-transfected Cos7 cells, and peptide-bound βTrCP1 was detected by immunoblotting. The unphosphorylated and phosphorylated IκBα peptides containing the conserved consensus βTrCP-binding sequence were used as controls. Fig. 5C shows that βTrCP1 barely bound the Cdc25B phospho-peptide under conditions where strong binding to the phosphorylated IκBα peptide was detected. Faint βTrCP1 signals that indicated binding to the doubly phosphorylated Cdc25B peptide were in fact detected

by longer exposure. Taken together, these results strongly support the idea that DAG is a critical sequence for JNK-induced Cdc25B ubiquitylation, but that the doubly phosphorylated DAGLCMDSPSP alone is insufficient for βTrCP binding.

The PEST-like sequence plays an important role in $SCF^{\beta TrCP}$-mediated Cdc25B ubiquitylation

Compared to Cdc25A, human Cdc25B possesses a longer PEST-like sequence that is rich in E (Glu) and S (Ser) but lacks P (Pro), and is located upstream from DAG (Fig. 1A). This PEST-like sequence may contribute to βTrCP binding because phosphorylation or the presence of acidic amino acids N-terminal to the consensus DSG/DDG sequences facilitates βTrCP binding (Jin *et al*., 2003; Kanemori *et al*., 2005; Westbrook *et al*., 2008). The PEST-like sequence in Cdc25B consists of 12 amino acids, which comprise three ESS units and one LSS unit. We mutated all eight Ser to non-phosphorylatable Ala to make S83/84/86/87/89/90/92/93A and examined its binding to βTrCP1. The $Cdc25B^{8SA}$ mutant (denoted "8SA (–PEST)" in Fig. 5) was unable to bind βTrCP1 and was resistant to JNK-induced degradation (Fig. 6A and S6A).

Next, we examined how many of the Cdc25B ESS/LSS sequences were necessary for βTrCP binding. We made a series of mutants with Ser-to-Ala mutations in the AA units, in which 2SA represents S83/84A, 4SA represents S83/84/86/87A, 6SA represents S86/87/89/90/92/93A, and 8SA is as described above (-PEST; see Fig. 6B) in the $Cdc25^{DAA}$ background. The βTrCP-binding activity of these mutants was roughly proportional to the number of intact SS sequences (Fig. 6B). Consistent with these results, the degree of JNK-dependent ubiquitylation decreased in Cdc25B that lacked SS sequences (Fig. 6C). Cdc25B with fewer SS sequences was more refractory to JNK-induced degradation (Fig. S6B). Of the four 2SA mutants (*i.e*., S83/84A, S86/87A, S89/90A, and S92/93A), the mutant with SS mutations closest to DAG (S92/93A) was the most refractory to JNK-induced degradation and the least ubiquitylated, suggesting that ESS phosphorylation closer to DAG is more important for degradation (S6C). The mutation in either E88 or E91 did not have any effect on JNK-induced degradation (Fig. S6D), excluding the possibility that the PEST-like sequence itself is a core βTrCP-binding site. Moreover, S101 and S103 is phosphorylated in $Cdc25B^{8SA}$, indication the phosphorylation of S101 and S103 independent of the PEST-like sequence (Fig. S6E). Collectively, these results clearly indicate that a PEST-like

sequence located upstream of DAG plays a critical role in $SCF^{\beta TrCP}$-mediated Cdc25B ubiquitylation.

A stretch of PEST-like sequence up to ^{101}SPSP of Cdc25B is a possible minimum sequence required for JNK-induced βTrCP binding

Next, we investigated the requirement of the PEST-like sequence and ^{101}SPSP in βTrCP binding. Given the difficulty synthesising Ser-rich peptides and their phosphorylated forms, we made GST-fused peptides running from ^{82}ESS to ^{101}SPSP and their phospho-mimetic mutants, purified them from *E. coli*, and investigated their binding to βTrCP1. The GST-fused peptides used were as follows: 10S (non-phosphorylated form), 8D2S (S-to-D mutation in the PEST-like sequence), 8S2D (^{101}DPDP mutant), and 10D (all S to D) (Fig. 7A). Such *E. coli*-produced proteins were mixed with Myc-βTrCP1-expressing Cos7 cell extracts in the presence of 1 μM staurosporine to avoid phosphorylation of the GST-fused peptides by the kinases in Cos7 cell extracts. Peptide-bound βTrCP1 was detected by immunoblotting. As expected, the βTrCP1 bound to the phospho-mimetic peptides, but not the unphosphorylated one (Fig. 7A). βTrCP1 bound strongly to GST-10D, and less strongly to 8D2S and 8S2D. No βTrCP1 binding was detected for the GST-10S peptide. These

results strongly suggest that the phosphorylation of Ser residues is required in the βTrCP-binding peptide consisting of ^{82}ESS to ^{101}SPSP.

Next, we examined the stability of the Cdc25B^{10D} mutant in HeLa cells. Cdc25B of wild type, 10D, 10A (all Ser residues in ^{82}ESS to ^{101}SPSP were replaced by non-phosphorylatable Ala), and D94A were transfected to HeLa cells and their expression was detected in the absence of stress. As indicated in Fig. 7B, the expression of the phospho-mimetic Cdc25B^{10D} mutant was less than that of the wild type, indicating that Cdc25B^{10D} is unstable, even under unstressed conditions, supporting the idea that full βTrCP binding requires phosphorylation.

Finally, we investigated the contribution of the DAG and DDG βTrCP-binding sites to Cdc25B stability in stressed and unstressed conditions. FLAG-Cdc25B of wild type, D94A, DAA, or D94A/DAA was transfected to HeLa cells and its expression was determined by immunoblotting. Typical expression of such mutants under anisomycin stress is shown in Fig. 8A. βTrCP1 binding to the Cdc25B mutant in the presence of JNK activity is also shown in Fig. S7. As expected, Cdc25B^{WT} and Cdc25B^{DAA} were susceptible to anisomycin treatment and Cdc25B^{D94A} was more refractory to it. The degradation of Cdc25B$^{D94A/DAA}$ was quite stable under anisomycin stress. These results indicate that the newly identified DAG βTrCP-binding sequence is responsible for

stress-induced Cdc25B degradation. We also investigated the stability of such Cdc25B proteins in the presence of cycloheximide to estimate their steady-state stability (Fig. 8B). $Cdc25B^{DAA}$ was more stable than $Cdc25B^{WT}$, but $Cdc25B^{D94A}$ was even more stable than $Cdc25B^{WT}$ or $Cdc25B^{DAA}$. Here again, the degradation of $Cdc25B^{D94A/DAA}$ was not observed with cycloheximide. These results suggest that the newly identified Cdc25B N-terminal βTrCP-binding region controls Cdc25B stability under both stressful and steady-state conditions and that the N-terminal DAG and constitutive DDG βTrCP binding sites cooperatively control Cdc25B stability.

Discussion

Previously, we showed that the cellular stresses that activate JNK or p38 induce Cdc25B degradation and that S101 and S103 are involved in Cdc25B stability (Uchida *et al.*, 2009). We also suggested the involvement of the ubiquitin–proteasome system in stress-induced Cdc25B degradation. In this report, we identified $SCF^{\beta TrCP}$ as the ubiquitin ligase responsible for non-genotoxic stress-induced Cdc25B degradation. Moreover, S101 and S103 are highly phosphorylated by such stresses and are involved in ubiquitylation by $SCF^{\beta TrCP}$.

Our results indicate that non-canonical ^{94}DAG and ^{101}SPSP in Cdc25B play important roles in Cdc25B for βTrCP binding. Moreover, an upstream PEST-like sequence starting from ^{82}ESS turned out to have a critical role in βTrCP binding to Cdc25B. Human Cdc25B has a longer PEST-like sequence than Cdc25A. The entire 12-amino-acid PEST-like sequence was essential for proper ubiquitylation. These results strongly indicate that the PEST-like sequence and SPSP cooperate with DAG for Cdc25B ubiquitylation under conditions that activate p38 and JNK. Moreover, the newly identified βTrCP-binding sequence around DAG is likely involved in steady-state Cdc25B degradation in collaboration with DDG under both stress-induced and steady-state conditions, given that the Cdc25B$^{D94A/DAA}$ double mutant was stable irrespective of cellular stress and SCF^{βTrCP} barely ubiquitylated Cdc25B$^{D94A/DAA}$. Hence, we safely conclude that Cdc25B stability is regulated mainly by SCF^{βTrCP}-mediated ubiquitylation via two independent sites: DAG and DAA.

The Ser residues in ^{101}SPSP, located downstream from ^{94}DAG, are highly phosphorylated upon JNK and p38 activation. In addition, a GST-fused phospho-mimetic peptide of ^{82}ESS to ^{101}SPSP bound βTrCP1, whereas that with the wild-type PEST-like sequence with SPSP did not, suggesting that the highly phosphorylated PEST-like sequence in Cdc25B is critical for βTrCP binding. These

results strongly suggest that full phosphorylation of the stretch from ^{82}ESS to ^{101}SPSP is required for Cdc25B to bind βTrCP. Such phosphorylation may confer a negative charge. The importance of phosphorylation in the upstream sequences to the core DSG sequence has also been reported in Cdc25A and REST (Jin *et al*., 2003; Westbrook *et al*., 2008). It was also reported that the stability of *Xenopus* Cdc25A is strongly affected by negatively charged amino acids surrounding the constitutive βTrCP-binding motif DDG (Kanemori *et al*., 2005). Hence, the βTrCP-binding motif-like DAG sequence in Cdc25B functions in βTrCP binding by virtue of the strong negative charge resulting from acidic residues, which may enable a strong interaction with βTrCP. Analysis of the crystal structure should confirm this.

Under non-genotoxic stress, the Ser residues of the SPSP sequence are preferentially phosphorylated by p38 and JNK. Interestingly, S101 was weakly but constitutively phosphorylated under steady-state conditions when both p38 and JNK were inactive. These results indicate that an unidentified proline-directed kinase(s) phosphorylates S101 in the steady-state condition, which may contribute to Cdc25B degradation during the interphase. In this context, Isoda *et al*. (2009) reported the inhibition of phosphorylation by the CDK inhibitor p21 in the corresponding Ser residue in *Xenopus* Cdc25A. Perhaps the interphase-specific CDK-cyclins that are

active from the G1 phase through the S phase, such as Cdk2-cyclin E, Cdk2-cyclin A, and possibly Cdk4-cyclin D, phosphorylate S101 to keep Cdc25B expression low. The identification of a kinase that phosphorylates Cdc25B S101 under steady-state conditions is likely important for understanding the post-translational regulation of Cdc25B. A need for phosphorylation in the Cdc25B PEST-like sequence for βTrCP binding was also suggested. Given that the phosphorylation of Ser residues in the PEST-like sequence is a prerequisite for βTrCP binding, it is also important to identify the kinase(s) responsible for a full understanding of Cdc25B regulation. More work is needed to understand the regulation of Cdc25B stability by phosphorylation under steady-state and stress-induced conditions.

In conclusion, we identified a new site in Cdc25B for non-genotoxic stress-induced βTrCP binding and proved that $SCF^{\beta TrCP}$ is the responsible ubiquitin ligase. The newly identified site is DAG, which is thought to be inactive in βTrCP binding; it is surrounded by an upstream PEST-like sequence and a downstream SPSP. Our results suggest that the full phosphorylation of the PEST-like sequence and SPSP are required for βTrCP binding and that the new site and the previously reported DDG constitutive βTrCP binding site collaboratively regulate the stability of Cdc25B under both stress-induced and steady-state conditions. Cdc25B and Cdc25A are

over-expressed in many tumours, and their overexpression is correlated with a poor prognosis (Kristjansdottir and Rudolph, 2004; Boutros *et al*., 2007). The uncontrolled expression of Cdc25B is itself toxic, as it induces premature entry into the M phase (Karlsson *et al*., 1999) and possibly genomic instability. Further studies that elucidate the regulation of Cdc25B stability should increase our understanding of the role of Cdc25B in cell cycle control and the contribution of the deregulation of Cdc25B stability to tumorigenesis.

Materials and Methods

Reagents and plasmids

Reagents of the highest grade were obtained from Wako (Osaka, Japan) or Sigma. The following siRNAs were purchased from Dharmacon: βTrCP1/βTrCP2 (denoted as pan-βTrCP siRNA in this report: Margottin-Goguet *et al*., 2003; Guardavaccaro *et al*., 2003), βTrCP1 (5'-UGACAACACUAUCAGAUUA-3'), and βTrCP2 (5'-GGACUUUAUUACCGCUUUA-3'). The validated stealth RNAi for JNK1 (5'-GGGCCUACAGAGAGCTAGUUCUUAU-3') and JNK2 (5'-GCCCAAGGGAUUGUUUGUGCUGCAU-3' and 5'-GCCAACUGUGAGGAAUUAUGUCGAA-3') were obtained from Invitrogen. The

siRNA for luciferase (5'-CGUACGCGGAAUACUUCGA-3') was obtained from QIAGEN. Anisomycin, SB202190, PD169316, and SP600125 were obtained from Calbiochem. The following cDNAs were used: human Cdc25B1, human Cdc25B3, mouse Cdc25B1, mouse p38α, mouse MKK6, mouse JNK1, mouse MKK7, human βTrCP1, human βTrCP2, human Skp1, human Skp2, human Cdc4, human Cul1, and mouse Rbx1. FLAG, HA, and Myc-tagged expression plasmids were constructed using the pEF6/Myc-His vector, which includes the EF1α promoter (Invitrogen), as described elsewhere (Uchida *et al*., 2004). The mutant versions of the above cDNAs were generated by PCR-based mutagenesis, and their nucleotide sequences were confirmed by sequencing.

Antibodies and proteins

Active JNK1 kinase was purchased from Invitrogen. The rabbit antibody specific for Cdc25B phospho-S101 was obtained from GenScript Corporation (USA) using NH_2-MD(PO_4-)SPSPMDPHMAEC-COOH as the antigen. The rabbit antibodies specific for phospho-S103 and phospho-S101/103 were obtained from IBL (Japan) using NH_2-MDSP(PO_4-)SPMDPHMAEC-COOH and NH_2-MD(PO_4-)SP(PO_4-)SPMDPHMAEC-COOH as the respective antigens. Each

anti-phospho-antibody was affinity purified with antigen peptide before use. The antibodies purchased were as follows: mouse anti-TrCP1 was purchased from Zymed; Cdc25A (F-6), Cdc25B (C-20), and JNK1 (C-17) antibodies were from Santa Cruz Biotechnology; and anti-actin, Myc-tag (9B11), HA-tag 262K, phospho-JNK-T183/Y185 (G9), MK2, c-Jun, and phospho-c-Jun-S63II were obtained from Cell Signaling. The anti-Cdc25B (AF1649) was obtained from R & D Systems. Secondary antibodies labelled with horseradish peroxidase were purchased from DAKO. Anti-FLAG-M2-agarose beads were purchased from Sigma. The rabbit anti-FLAG serum was raised in house. *E. coli*-produced GST-fused Cdc25B peptides encompassing ^{82}ESS to ^{101}SPSP and the phospho-mimetic mutant versions were purified from IPTG-induced BL21 cells with glutathione beads (GE Healthcare).

Cells, cell culture, and siRNA or plasmid transfection

HeLa and Cos7 cells were grown in Dulbecco's modified Eagle's medium (DMEM) containing high glucose (Sigma) supplemented with 10% foetal bovine serum (FBS; Hyclone) and antibiotics. HeLa-W40 cells that constitutively expressed FLAG-tagged wild-type Cdc25B under the EF1α promoter were also cultured under the same conditions (Uchida *et al*., 2009). We also isolated HeLa cells constitutively expressing

the FLAG-tagged Cdc25B^{DAA} mutant (HeLa-DAA34 cells). In these cells, the expression of external Cdc25B was roughly 20 to 40-fold higher than that of endogenous Cdc25B. Plasmids were transiently transfected with Lipofectamine 2000 (Invitrogen). The amount of plasmid DNA used for transfection was about 500 ng for a 6-well plate. HeLa and Cos7 cells were used for assays of stability (degradation) and for protein-protein interaction, respectively. The siRNA was transfected using Lipofectamine RNAiMAX (Invitrogen).

Biochemical methods and in vitro *ubiquitylation assay*

Crude extraction for protein analysis followed by immunoblotting or immunoprecipitation was performed as described previously (Uchida *et al*., 2004). The *in vitro* ubiquitylation assay was performed essentially as described previously (Watanabe *et al*., 2004). Briefly, HA-tagged Rbx1, Skp2, and Cul1, and c-Myc-tagged F-box proteins were co-expressed in Cos7 cells, and the SCF complex was recovered by immunoprecipitation with anti-c-Myc-agarose (MBL, Japan). ^{35}S-methionine-labelled Cdc25B was prepared with a TNT-coupled transcription and translation system (Promega). The reaction mixture in a total volume of 20 μL contained SCF complex on beads, ^{35}S-labelled Cdc25B (2 μL), 20 μg bovine ubiquitin (Sigma), 0.8 μg human

recombinant E1 enzyme (BIOMOL), 1 µg human 6xHis-Ubc5 (Wako, Osaka, Japan), and an ATP-regenerating system (2 mM ATP, 10 mM creatine phosphate, 0.35 U/ml creatine kinase, 0.6 U/mL inorganic pyrophosphatase), supplemented with 5 µM MG132, 0.5 µM okadaic acid, and 1 µM ubiquitin-aldehyde (Boston Biochem). When necessary, recombinant active JNK1 (25 ng) was added to the reaction. The mixtures were incubated at 37°C for 2 h, followed by sodium dodecyl sulphate-polyacrylamide gel electrophoresis (SDS-PAGE) in a 2–15% gradient gel, and the ubiquitylated Cdc25B was visualised using the FUJI BAS system.

Acknowledgements

We thank S. I. Reed (Scripps Institute) for the generous gift of human Cdc4 plasmids. This work was supported by grants from the following institutions: The Ministry of Health, Labour and Welfare of Japan, the Ministry of Culture, Sports, Science and Technology of Japan, the Research Grants Council of Hong Kong, the Cosmetology Research Foundation, the Long-range Research Initiative (LRI) of the Japan Chemical Industry Association, and the Japan Science and Technology Agency.

References

Baldin, **V**., **Cans**, **C**., **Superti-Furga**, **G**., **and Ducommun**, **B**. (1997). Alternative splicing of the human CDC25B tyrosine phosphatase. Possible implications for growth control? *Oncogene* **14**, 2485-2495.

Bartek, **J**., **Lukas**, **C**., **and Lukas**, **J**. (2004). Checking on DNA damage in S phase. *Nat*. *Rev*. *Mol*. *Cell Biol*. **5**, 792-804.

Boutros, **R**., **Dozier**, **C**., **and Ducommun**, **B**. (2006). The when and wheres of CDC25 phosphatases. *Curr*. *Opin*. *Cell Biol*. **18**, 185-191.

Boutros, **R**., **Lobjois**, **V**., **and Ducommun**, **B**. (2007). CDC25 phosphatases in cancer cells: key players? Good targets? *Nat*. *Rev*. *Cancer* **7**, 495-507.

Busino, **L**., **Chiesa**, **M**., **Draetta**, **G**. **F**., **and Donzelli**, **M**. (2004). Cdc25A phosphatase: combinatorial phosphorylation, ubiquitylation and proteolysis. *Oncogene* **23**, 2050-2056.

Busino, **L**., **Donzelli**, **M**., **Chiesa**, **M**., **Guardavaccaro**, **D**., **Ganoth**, **D**., **Dorrello**, **N**. **V**., **Hershko**, **A**., **Pagano**, **M**., **and Draetta**, **G**. **F**. (2003). Degradation of Cdc25A by beta-TrCP during S phase and in response to DNA damage. *Nature* 426, 87-91.

Chen, **M**. **S**., **Hurov**, **J**., **White**, **L**. **S**., **Woodford-Thomas**, **T**., **and Piwnica-Worms**, **H**. (2001). Absence of apparent phenotype in mice lacking Cdc25C protein phosphatase. *Mol*. *Cell*. *Biol*. **21**, 3853-3861.

Donzelli, **M**., **and Draetta**, **G**. **F**. (2003). Regulating mammalian checkpoints through Cdc25 inactivation. *EMBO Rep*. **4**, 671-677.

Ferguson, **A**. **M**., **White**, **L**. **S**., **Donovan**, **P**. **J**., **and Piwnica-Worms**, **H**. (2005). Normal cell cycle and checkpoint responses in mice and cells lacking Cdc25B and Cdc25C protein phosphatases. *Mol*. *Cell*. *Biol*. **25**, 2853-2860.

Frescas, **D**., **and Pagano**, **M**. (2008). Deregulated proteolysis by the F-box proteins SKP2 and beta-TrCP: tipping the scales of cancer. *Nat*. *Rev*. *Cancer* **8**, 438-449.

Galaktionov, **K**., **Lee**, **A**. **K**., **Eckstein**, **J**., **Draetta**, **G**., **Meckler**, **J**., **Loda**, **M**., **and Beach**, **D**. (1995). CDC25 phosphatases as potential human oncogenes. *Science* 269, 1575-1577.

Guardavaccaro, **D**., **Kudo**, **Y**., **Boulaire**, **J**., **Barchi**, **M**., **Busino**, **L**., **Donzelli**, **M**., **Margottin-Goguet**, **F**., **Jackson**, **P**. **K**., **Yamasaki**, **L**., **and Pagano**, **M**. (2003). Control of meiotic and mitotic progression by the F box protein beta-Trcp1 *in vivo*. *Dev*. *Cell* 4, 799-812.

Isoda, **M**., **Kanemori**, **Y**., **Nakajo**, **N**., **Uchida**, **S**., **Yamashita**, **K**., **Ueno**, **H**., **and Sagata**, **N**. (2009). The extracellular signal-regulated kinase-mitogen-activated protein kinase pathway phosphorylates and targets Cdc25A for $SCF^{beta\text{-}TrCP}$-dependent degradation for cell cycle arrest. *Mol*. *Biol*. *Cell* **20**, 2186-2195.

Jin, **J**., **Shirogane**, **T**., **Xu**, **L**., **Nalepa**, **G**., **Qin**, **J**., **Elledge**, **S**. **J**., **and Harper**, **J**. **W**. (2003). $SCF^{beta\text{-}TrCP}$ links Chk1 signaling to degradation of the Cdc25A protein phosphatase. *Genes Dev*. **17**, 3062-3074.

Kakizuka, **A**., **Sebastian**, **B**., **Borgmeyer**, **U**., **Hermans-Borgmeyer**, **I**., **Bolado**, **J**., **Hunter**, **T**., **Hoekstra**, **M**. **F**., **and Evans**, **R**. **M**. (1992). A mouse cdc25 homolog is differentially and developmentally expressed. *Genes Dev*. 6, 578-590.

Kanemori, **Y**., **Uto**, **K**., **and Sagata**, **N**. (2005). Beta-TrCP recognizes a previously undescribed nonphosphorylated destruction motif in Cdc25A and Cdc25B phosphatases. *Proc*. *Natl*. *Acad*. *Sci*. *USA* **102**, 6279-6284.

Karlsson, **C**., **Katich**, **S**., **Hagting**, **A**., **Hoffmann**, **I**., **and Pines**, **J**. (1999). Cdc25B and Cdc25C differ markedly in their properties as initiators of mitosis. *J*. *Cell Biol*. **146**, 573-584.

Kristjansdottir, **K**., **and Rudolph**, **J**. (2004). Cdc25 phosphatases and cancer. *Chem*. *Biol*. **11**, 1043-1051.

Latres, **E**., **Chiaur**, **D**. **S**., **and Pagano**, **M**. (1999). The human F box protein beta-TrCP associates with the Cul1/Skp1 complex and regulates the stability of beta-catenin. *Oncogene* **18**, 849-854.

Lee, **G**., **White**, **L**. **S**., **Hurov**, **K**. **E**., **Stappenbeck**, **T**. **S**., **and Piwnica-Worms**, **H**. (2009). Response of small intestinal epithelial cells to acute disruption of cell division through CDC25 deletion. *Proc*. *Natl*. *Acad*. *Sci*. *USA* **106**, 4701-4706.

Lincoln, **A**. **J**., **Wickramasinghe**, **D**., **Stein**, **P**., **Schultz**, **R**. **M**., **Palko**, **M**. **E**., **De Miguel**, **M**. **P**., **Tessarollo**, **L**., **and Donovan**, **P**. **J**. (2002). Cdc25b phosphatase is required for resumption of meiosis during oocyte maturation. *Nat*. *Genet*. 30, 446-449.

Ma, **Z**. **Q**., **Chua**, **S**. **S**., **DeMayo**, **F**. **J**., **and Tsai**, **S**. **Y**. (1999). Induction of mammary gland hyperplasia in transgenic mice over-expressing human Cdc25B. *Oncogene* **18**, 4564-4576.

Margottin-Goguet, **F**., **Hsu**, **J**. **Y**., **Loktev**, **A**., **Hsieh**, **H**. **M**., **Reimann**, **J**. **D**., **and Jackson**, **P**. **K**. (2003). Prophase destruction of Emi1 by the $SCF^{betaTrCP/Slimb}$ ubiquitin ligase activates the anaphase promoting complex to allow progression beyond prometaphase. *Dev*. *Cell* **4**, 813-826.

Melixetian, **M**., **Klein**, **D**. **K**., **Sorensen**, **C**. **S**., **and Helin**, **K**. (2009). NEK11 regulates CDC25A degradation and the IR-induced G2/M checkpoint. *Nat*. *Cell*. *Biol*. **11**, 1247-1253.

Miyata, **H**., **Doki**, **Y**., **Yamamoto**, **H**., **Kishi**, **K**., **Takemoto**, **H**., **Fujiwara**, **Y**., **Yasuda**, **T**., **Yano**, **M**., **Inoue**, **M**., **Shiozaki**, **H**. *et al*. (2001). Overexpression of CDC25B overrides radiation-induced G2-M arrest and results in increased apoptosis in esophageal cancer cells. *Cancer Res*. **61**, 3188-3193.

Morgan, **D**. **O**. (1995). Principles of CDK regulation. *Nature* **374**, 131-134.

Ray, **D**., **Terao**, **Y**., **Nimbalkar**, **D**., **Hirai**, **H**., **Osmundson**, **E**. **C**., **Zou**, **X**., **Franks**, **R**., **Christov**, **K**., **and Kiyokawa**, **H**. (2007). Hemizygous disruption of Cdc25A inhibits cellular transformation and mammary tumorigenesis in mice. *Cancer Res*. **67**, 6605-6611.

Seki, **A**., **Coppinger**, **J**. **A**., **Du**, **H**., **Jang**, **C**. **Y**., **Yates**, **J**. **R**., **3rd and Fang**, **G**. (2008). Plk1- and beta-TrCP-dependent degradation of Bora controls mitotic progression. *J*. *Cell Biol*. **181**, 65-78.

Uchida, **S**., **Kuma**, **A**., **Ohtsubo**, **M**., **Shimura**, **M**., **Hirata**, **M**., **Nakagama**, **H**., **Matsunaga**, **T**., **Ishizaka**, **Y**., **and Yamashita**, **K**. (2004). Binding of 14-3-3beta but not 14-3-3sigma controls the cytoplasmic localization of CDC25B: binding site

preferences of 14-3-3 subtypes and the subcellular localization of CDC25B. *J. Cell Sci*. **117**, 3011-3020.

Uchida, **S**., **Yoshioka**, **K**., **Kizu**, **R**., **Nakagama**, **H**., **Matsunaga**, **T**., **Ishizaka**, **Y**., **Poon**, **R**. **Y**., **and Yamashita**, **K**. (2009). Stress-activated mitogen-activated protein kinases c-Jun NH2-terminal kinase and p38 target Cdc25B for degradation. *Cancer Res*. **69**, 6438-6444.

Watanabe, **N**., **Arai**, **H**., **Nishihara**, **Y**., **Taniguchi**, **M**., **Hunter**, **T**., **and Osada**, **H**. (2004). M-phase kinases induce phospho-dependent ubiquitination of somatic Wee1 by $SCF^{beta\text{-}TrCP}$. *Proc. Natl. Acad. Sci. USA* **101**, 4419-4424.

Westbrook, **T**. **F**., **Hu**, **G**., **Ang**, **X**. **L**., **Mulligan**, **P**., **Pavlova**, **N**. **N**., **Liang**, **A**., **Leng**, **Y**., **Maehr**, **R**., **Shi**, **Y**., **Harper**, **J**. **W**. *et al*. (2008). $SCF^{beta\text{-}TrCP}$ controls oncogenic transformation and neural differentiation through REST degradation. *Nature* **452**, 370-374.

Winston, **J**. **T**., **Strack**, **P**., **Beer-Romero**, **P**., **Chu**, **C**. **Y**., **Elledge**, **S**. **J**., **and Harper**, **J**. **W**. (1999). The $SCF^{beta\text{-}TrCP}$-ubiquitin ligase complex associates specifically with phosphorylated destruction motifs in IκBα and β-catenin and stimulates IκBα ubiquitination *in vitro*. *Genes Dev*. **13**, 270-283.

Wu, **G**., **Xu**, **G**., **Schulman**, **B**. **A**., **Jeffrey**, **P**. **D**., **Harper**, **J**. **W**., **and Pavletich**, **N**. **P**. (2003). Structure of a beta-TrCP1-Skp1-beta-catenin complex: destruction motif binding and lysine specificity of the $SCF^{beta\text{-}TrCP1}$ ubiquitin ligase. *Mol*. *Cell*. **11**, 1445-1456.

Yao, **Y**., **Slosberg**, **E**. **D**., **Wang**, **L**., **Hibshoosh**, **H**., **Zhang**, **Y**. **J**., **Xing**, **W**. **Q**., **Santella**, **R**. **M**., **and Weinstein**, **I**. **B**. (1999). Increased susceptibility to carcinogen-induced mammary tumors in MMTV-Cdc25B transgenic mice. *Oncogene* **18**, 5159-5166.

Figure legends

Figure 1. βTrCP binds Cdc25B. (A) The aligned amino acid sequences of human and mouse Cdc25B corresponding to that of human Cdc25A required for βTrCP binding. Asterisks indicate amino acids common to all three peptides. (B) Each FLAG-tagged cDNA of human Cdc25B1 and B3 and mouse Cdc25B1 was cotransfected with either JNK1 and its activator MKK7 or p38α and its activator MKK6, followed by immunoblotting to detect the expression of the indicated proteins (JNK1 or p38α was cotransfected with its respective activator, MKK7 or MKK6, unless stated otherwise and the coexpression of JNK1 and MKK7 or p38α with MKK6 is shown as JNK1 or p38, respectively, thereafter). The expression of human Cdc25B1 with a mutation at D94 to A of DAG (D94A) was also determined. (C) Either a FLAG-Cdc25B^{WT} or Cdc25B^{DAA} with mutations in the constitutive βTrCP-binding sequence DDG was cotransfected with Myc-βTrCP1 in the presence or absence of JNK1. Then, 24 h later, either Cdc25B binding to βTrCP1 or recovered Cdc25B was determined by immunoprecipitation with anti-FLAG beads, followed by immunoblotting with anti-Myc or anti-FLAG antibodies (Cdc25B-IP panel). The expression of the indicated proteins is also shown (WCE panel). (D) The βTrCP1 binding to Cdc25B fragments of the N-terminal 175 amino acids (1–175, 25B–N) or C-terminal fragment (180–580,

25B–C), both of which contain an N-terminal FLAG-tag and C-terminal GFP-tag, was examined as described in (C). FLAG-GFP was used as a control (Cdc25B-IP panel). The expression of the indicated proteins is shown (WCE panel). (E) FLAG-Cdc25B^{DAA} and Myc-tagged F-box proteins were cotransfected and their interaction was determined by immunoprecipitation and immunoblotting. The interaction between Cdc25B^{DDA} and βTrCP1$^{\Delta F}$ lacking an F-box sequence (17) was also determined (Cdc25B-IP panel). The expression of the indicated proteins is also shown (WCE panel).

Figure 2. **Cdc25B is ubiquitylated by SCF$^{\beta TrCP}$ *in vitro***. (A) ^{35}S-methionine-labelled Cdc25B^{DAA} was incubated with each SCF complex in the presence or absence of JNK1, and ubiquitylation was determined as described in the *Materials and Methods*. (B) ^{35}S-methionine-labelled Cdc25B^{DAA} was incubated with each SCF$^{\beta TrCP1}$ or SCF$^{\Delta\beta TrCP1}$ complex in the presence or absence of JNK1, and ubiquitylation was determined as described in (A). (C) SCF$^{\beta TrCP1}$-mediated ubiquitylation of ^{35}S-methionine-labelled Cdc25B^{WT} (wild type) or Cdc25B^{DAA} was determined as described in (A). (D) ^{35}S-methionine-labelled Cdc25B^{DAA} of S101/103 (wild type), or with a mutation of S101A, S103A, or S101/103A, was incubated with SCF$^{\beta TrCP1}$ to determine ubiquitylation as described in (A).

Figure 3. **βTrCP1/2 depletion stabilises Cdc25B**. (A) HeLa cells were depleted of both βTrCP1 and 2 with siRNA (either pan-βTrCP or combined siRNA for βTrCP1 and 2). Luci indicates siRNA against luciferase used as a control. After 24 h, HeLa cells were treated with 50 ng/ml anisomycin for 30 min. The expression of endogenous Cdc25B was determined by immunoprecipitation followed by immunoblotting. The expression of the indicated proteins was determined by immunoblotting. (B) HeLa-W40 cells transfected with either siRNA for Luci or pan-βTrCP were treated with cycloheximide (CHX, 50 μg/mL), and expression of the indicated proteins was determined by immunoblotting at the indicated times. The relative Cdc25B expression is shown in the lower panel with the value at time 0 set at 100. The bars indicate the standard deviation (SD) of three independent experiments. (C) The expression of $Cdc25B^{DAA}$ in HeLa-DAA34 cells in the presence of CHX was determined as described in (B). (D) HeLa-W40 cells transfected with either siRNA for Luci or pan-βTrCP were treated with 50 ng/mL anisomycin, and the expression of the indicated proteins was determined as described in (B).

Figure 4. **Cdc25B S101 and S103 are phosphorylated by non-genotoxic insults**. (A) HeLa-W40 cells that expressed FLAG-Cdc25B were treated with 50 ng/mL anisomycin. At the indicated times, Cdc25B was immunoprecipitated, and phosphorylation was detected with antibodies. The expression of FLAG-Cdc25B, c-Jun, MK2, and β-actin are also shown. (B) HeLa-W40 cells were treated with 300 mM NaCl, and phosphorylation at S101 and S103 and the expression of the indicated proteins was detected, as described in (A). (C) HeLa-W40 cells were treated with each inhibitor (5 μM each of SB202190 and PD169316 for p38 and 20 μM SP600125 for JNK, or a combination of SB and SP or PD and SP to inhibit p38 and JNK) 1 h before the 50 ng/mL anisomycin challenge. Cell extracts were prepared at 10 min, followed by the immunoprecipitation of Cdc25B. Phosphorylation at S101 and S103 and the expression of the indicated proteins were determined by immunoblotting. (D) HeLa-W40 cells were treated with siRNA for Luc or JNK (the siRNA for JNK was a mixture of one siJNK1 and two siJNK2). After 24 h, the cells were treated with 50 ng/mL anisomycin for 10 min and cell extracts were prepared. The phosphorylation of Cdc25B at S101 and S103 and the expression of the indicated proteins were determined by immunoblotting.

Figure 5. **Cdc25B peptide from ^{94}DAG to ^{101}SPSP is essential, but not sufficient, for Cdc25B ubiquitylation by SCF$^{\beta TrCP}$**. (A) FLAG-Cdc25B of the wild type or indicated mutants was cotransfected with Myc-βTrCP1 in the presence or absence of JNK1. Then, 24 h later, Cdc25B-bound βTrCP1 was detected by the immunoprecipitation of Cdc25B, followed by immunoblotting (Cdc25B-IP panel). The expression of the indicated proteins is also shown (WCE panel). (B) *In vitro* ubiquitylation by SCF$^{\beta TrCP1}$ of Cdc25B^{DAA} with wild-type DAG, or G96A or S101/103A mutations was determined, as described in Fig. 2A. (C) Phosphorylated or unphosphorylated Cdc25B peptides based on DAGLCMDSPSP that was conjugated with agarose beads was incubated with Myc-βTrCP1-expressing Cos7 cell extracts and the βTrCP1 bound to peptides was detected by immunoblotting.

Figure 6. **The PEST-like sequence is required for efficient ubiquitylation of Cdc25B**. (A) The following FLAG-Cdc25B^{DAA}-based mutants were cotransfected with Myc-βTrCP1 in the presence or absence of JNK1: WT with an intact PEST-like sequence; 8SA (-PEST) with mutations of eight serine residues in the PEST-like sequence to alanine; S101/103A; or D94A. After 24 h, Cdc25B was immunoprecipitated, and Cdc25B-bound βTrCP1 was detected by immunoblotting

(Cdc25B-IP panel). The expression of the indicated proteins was also determined (WCE panel). (B) FLAG-Cdc25B^{DAA} with an intact PEST-like sequence (WT) or with SS to AA mutations of two serine residues in three ESS units or one LSS unit was cotransfected with Myc-βTrCP1 in the presence or absence of JNK. The Cdc25B-bound βTrCP1 and protein expression are shown as indicated in (A). Cdc25B^{D94A} was used as a negative control. (C) The ^{35}S-labelled Cdc25B^{DAA}-based proteins used in (B) were processed to detect *in vitro* ubiquitylation, as described in Fig. 2A.

Figure 7. **A peptide encompassing ^{82}ESS to ^{101}SPSP is a possible βTrCP-binding sequence in Cdc25B**. (A) GST-fused Cdc25B-derived peptides consisting of ^{82}ESS to ^{101}SPSP were mixed with crude cell extracts prepared from Myc-tagged βTrCP1-transfected Cos7 cells, and this was followed by the recovery of proteins bound to GST-fused peptides. The recovered βTrCP1 was detected with anti-Myc antibody. The reaction mixture included 1 μM staurosporine to avoid the phosphorylation of Ser residues in the peptides by kinases present in the cell extracts. (B) FLAG-Cdc25B of wild type, 10D (all Ser residues in ^{82}ESS to ^{101}SPSP were replaced with Asp), 10A (all Ser residues in ^{82}ESS to ^{101}SPSP were replaced with Ala), or D94A was transfected to HeLa cells and their expression was determined by immunoblotting.

Figure 8. **DAG and DDG collaboratively regulate Cdc25B stability**. FLAG-tagged $Cdc25B^{WT}$, $Cdc25B^{D94A}$, $Cdc25B^{DAA}$, or $Cdc25B^{D94A/DAA}$ was transfected to HeLa cells, which were treated with 100 ng/mL anisomycin (panel A) or 50 μg/mL cycloheximide (panel B) 24 h after transfection. Crude cell extracts were prepared at the indicated times and the expression of Cdc25B, c-Jun, and β-actin was determined by immunoblotting. The relative Cdc25B expression is also shown with the value at time 0 set to 100. The bars indicated the SD of five independent experiments. In (A) and (B), the relative densitometric values of the expression of $Cdc25B^{WT}$, $Cdc25B^{D94A}$, $Cdc25B^{DAA}$, and $Cdc25B^{D94A/DAA}$ were 1, 1.98 ± 0.79, 1.77 ± 0.59, and 4.21 ± 1.2, respectively.

Fig. 1

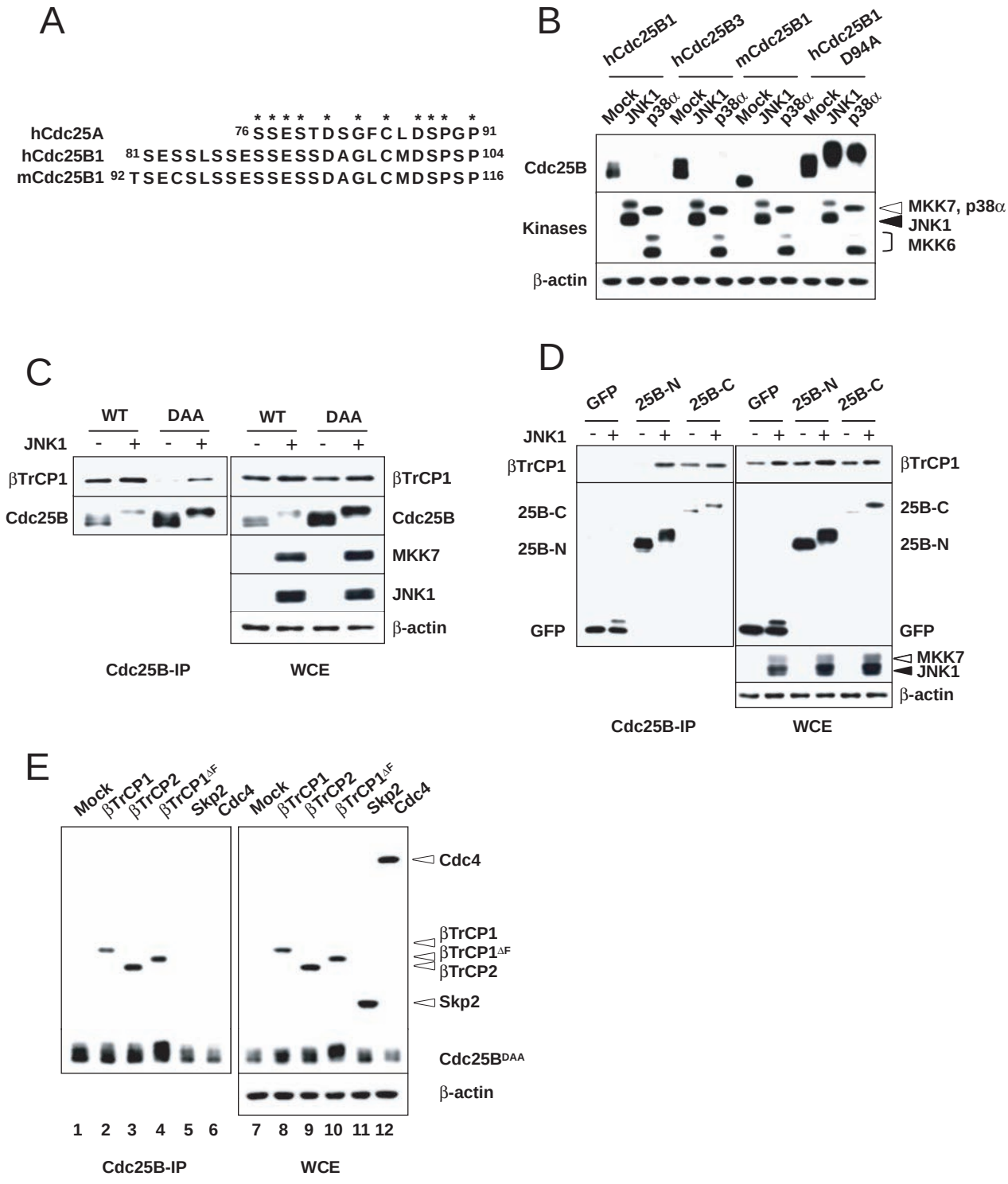
A
hCdc25A 76 S S E S T D S G F C L D S P G P 91
hCdc25B1 81 S E S S L S S E S S E S S D A G L C M D S P S P 104
mCdc25B1 92 T S E C S L S S E S S E S S D A G L C M D S P S P 116
B
hCdc25B1
hCdc25B3
mCdc25B1
hCdc25B1 D94A
Mock
JNK1
p38α
Cdc25B
Kinases
β-actin
MKK7, p38α
JNK1
MKK6
C
WT
DAA
JNK1
βTrCP1
Cdc25B
MKK7
JNK1
β-actin
Cdc25B-IP
WCE
D
GFP
25B-N
25B-C
JNK1
βTrCP1
25B-C
25B-N
GFP
MKK7
JNK1
β-actin
Cdc25B-IP
WCE
E
Mock
βTrCP1
βTrCP2
βTrCP1ΔF
Skp2
Cdc4
Cdc4
βTrCP1
βTrCP1ΔF
βTrCP2
Skp2
Cdc25BDAA
β-actin
1 2 3 4 5 6 7 8 9 10 11 12
Cdc25B-IP
WCE

Fig.2

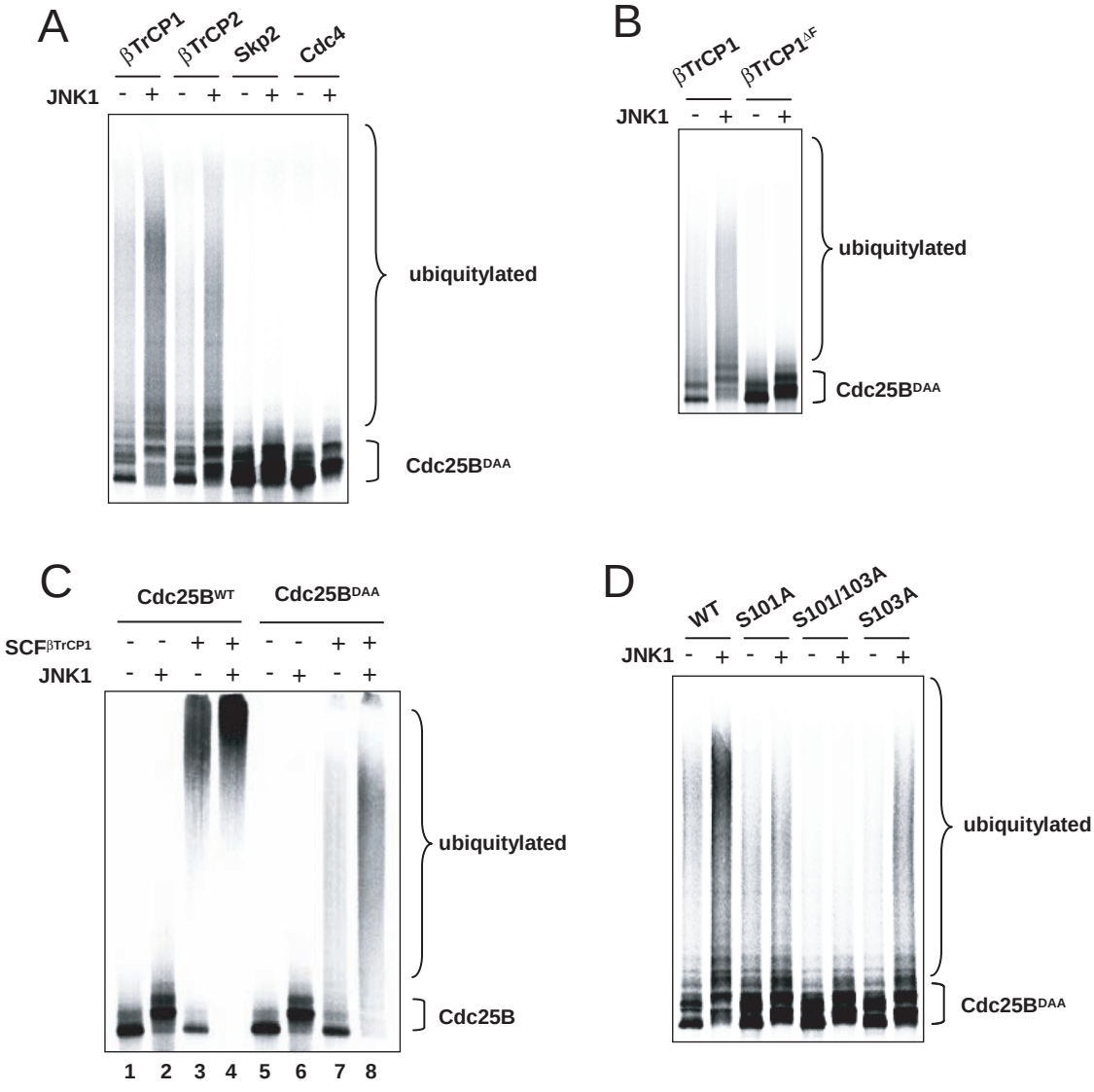
A
βTrCP1
βTrCP2
Skp2
Cdc4
JNK1 - + - + - + - +
ubiquitylated
Cdc25B^DAA
B
βTrCP1
βTrCP1^ΔF
JNK1 - + - +
ubiquitylated
Cdc25B^DAA
C
Cdc25B^WT
Cdc25B^DAA
SCF^βTrCP1 - - + + - - + +
JNK1 - + - + - + - +
ubiquitylated
Cdc25B
1 2 3 4 5 6 7 8
D
WT
S101A
S101/103A
S103A
JNK1 - + - + - + - +
ubiquitylated
Cdc25B^DAA

Fig.3

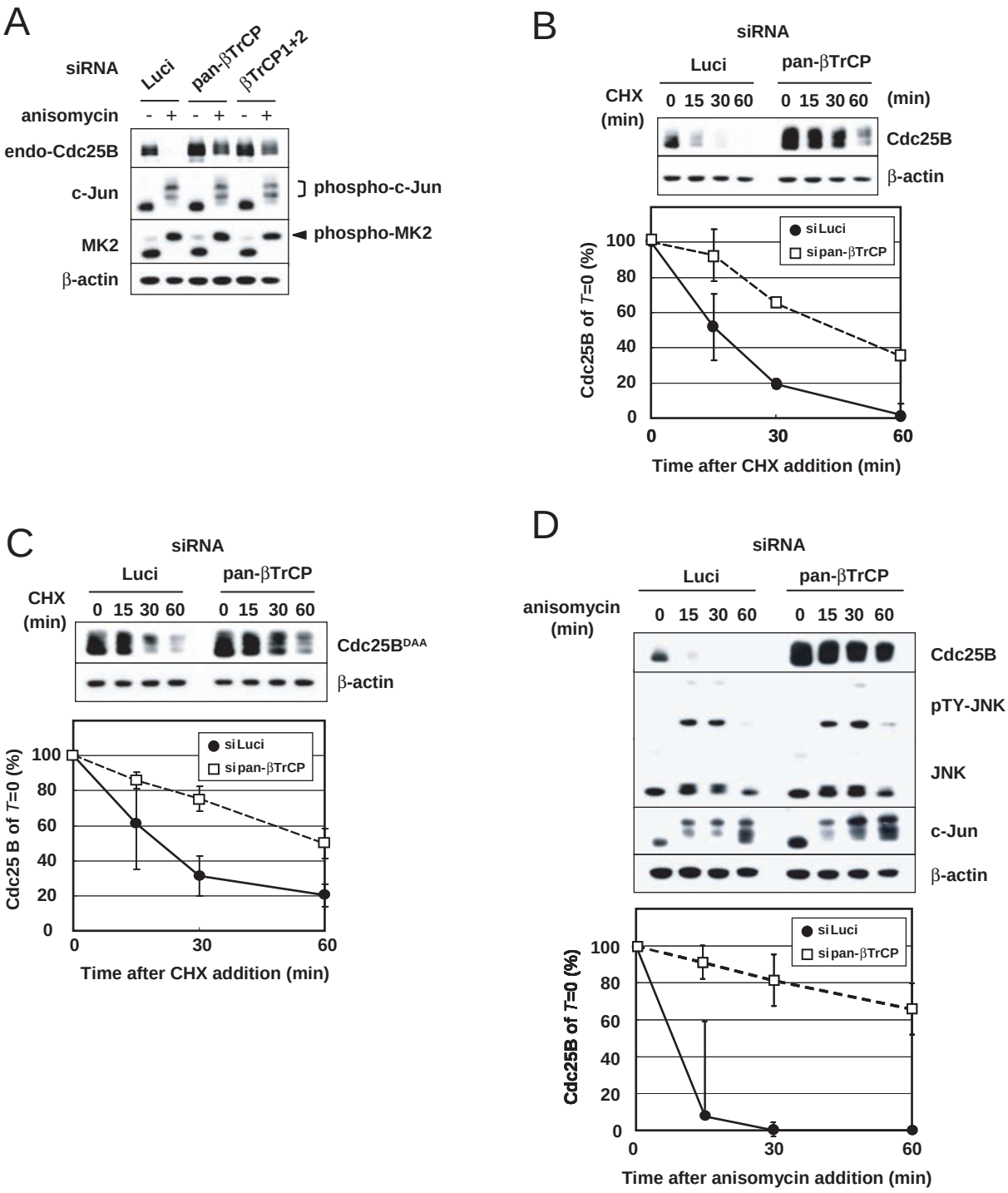
A
siRNA
Luci
pan-βTrCP
βTrCP1+2
anisomycin
- + - + - +
endo-Cdc25B
c-Jun
phospho-c-Jun
MK2
phospho-MK2
β-actin
B
siRNA
Luci
pan-βTrCP
CHX (min)
0 15 30 60 0 15 30 60 (min)
Cdc25B
β-actin
siLuci
sipan-βTrCP
Cdc25B of T=0 (%)
Time after CHX addition (min)
C
siRNA
Luci
pan-βTrCP
CHX (min)
0 15 30 60 0 15 30 60
Cdc25B^DAA
β-actin
siLuci
sipan-βTrCP
Cdc25 B of T=0 (%)
Time after CHX addition (min)
D
siRNA
Luci
pan-βTrCP
anisomycin (min)
0 15 30 60 0 15 30 60
Cdc25B
pTY-JNK
JNK
c-Jun
β-actin
siLuci
sipan-βTrCP
Cdc25B of T=0 (%)
Time after anisomycin addition (min)

Fig.4

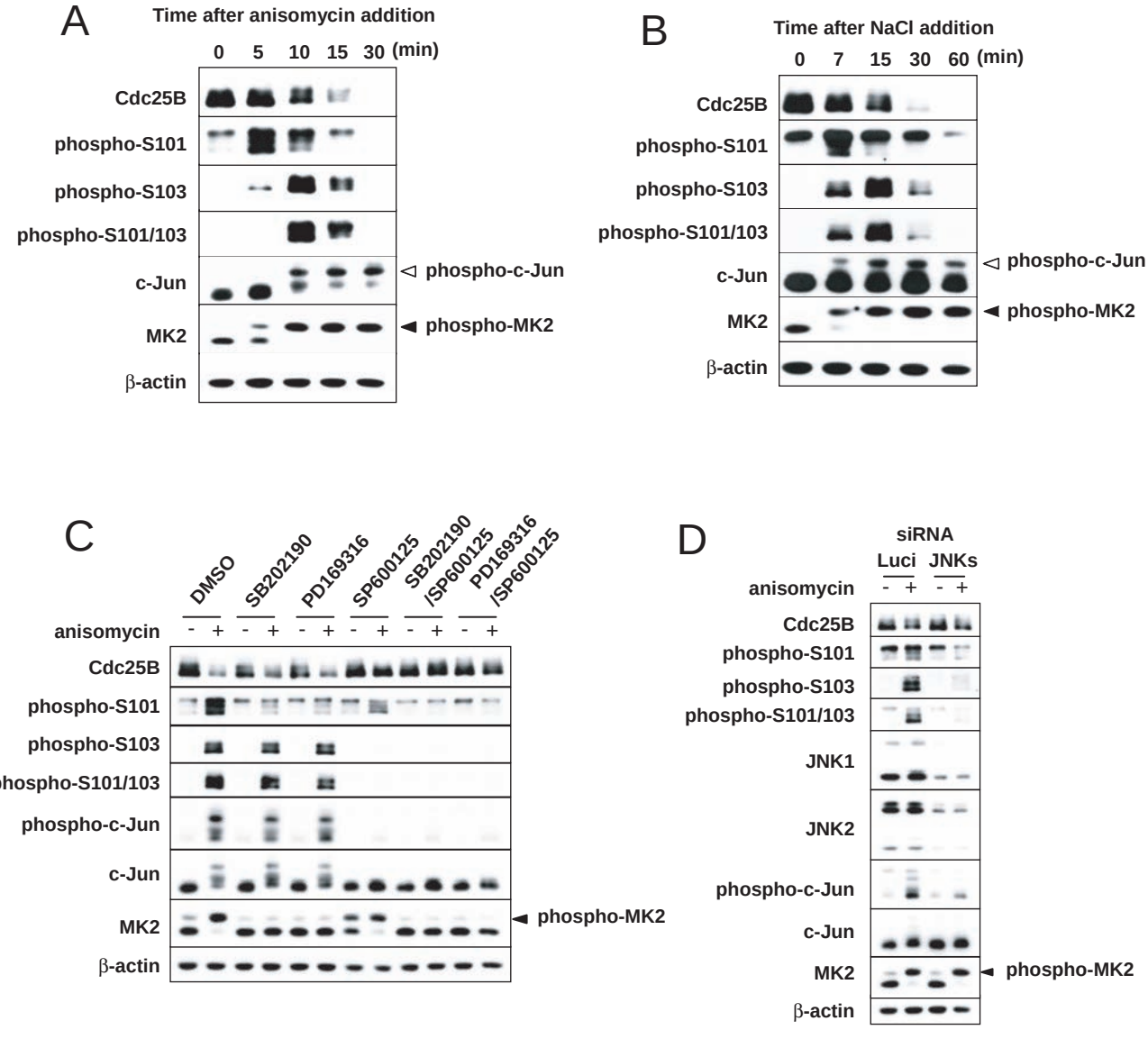
A
Time after anisomycin addition
0 5 10 15 30 (min)
Cdc25B
phospho-S101
phospho-S103
phospho-S101/103
c-Jun
MK2
β-actin
◁ phospho-c-Jun
◀ phospho-MK2
B
Time after NaCl addition
0 7 15 30 60 (min)
Cdc25B
phospho-S101
phospho-S103
phospho-S101/103
c-Jun
MK2
β-actin
◁ phospho-c-Jun
◀ phospho-MK2
C
DMSO
SB202190
PD169316
SP600125
SB202190 /SP600125
PD169316 /SP600125
anisomycin - + - + - + - + - + - +
Cdc25B
phospho-S101
phospho-S103
phospho-S101/103
phospho-c-Jun
c-Jun
MK2
β-actin
◀ phospho-MK2
D
siRNA
Luci JNKs
anisomycin - + - +
Cdc25B
phospho-S101
phospho-S103
phospho-S101/103
JNK1
JNK2
phospho-c-Jun
c-Jun
MK2
β-actin
◀ phospho-MK2

Fig.5

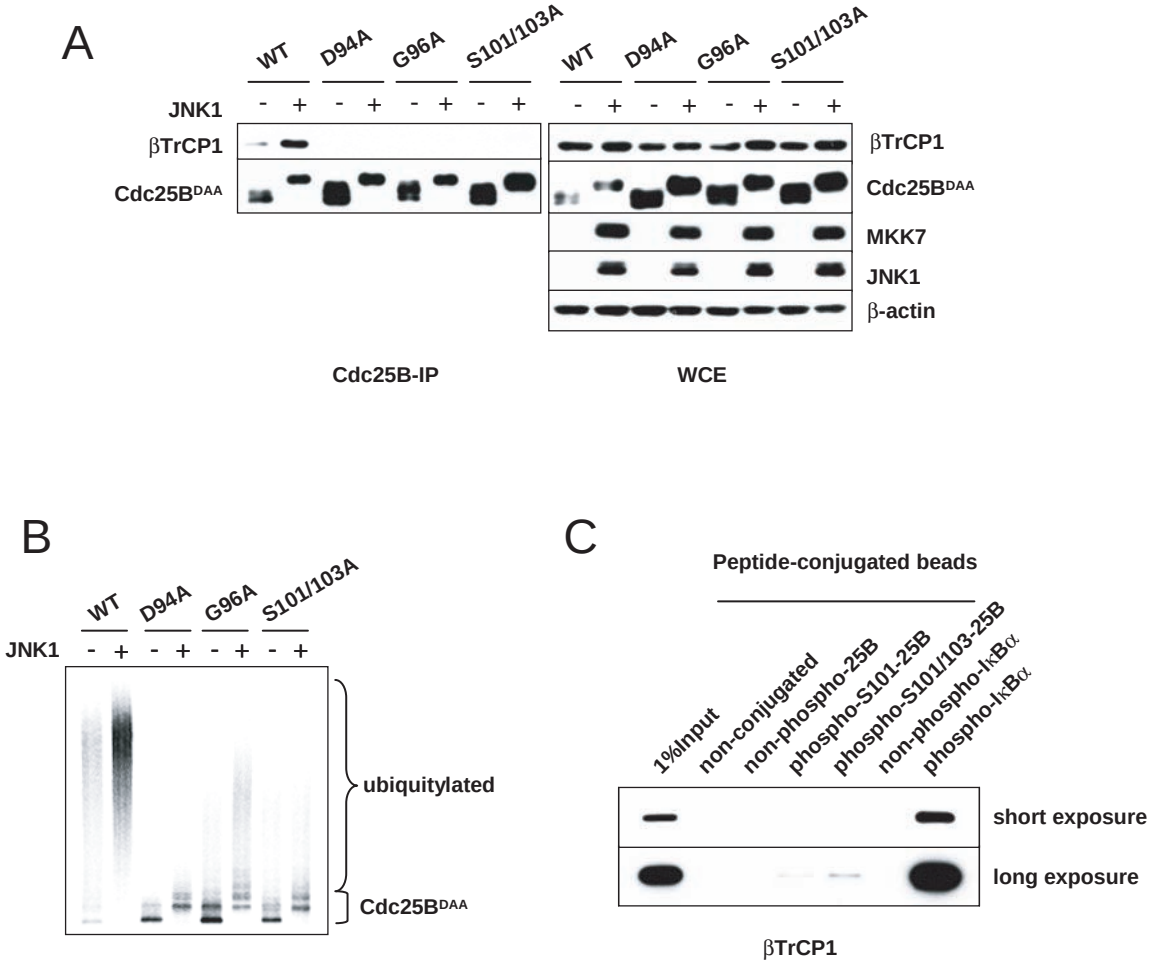
A
WT
D94A
G96A
S101/103A
WT
D94A
G96A
S101/103A
JNK1
- + - + - + - + - + - + - + - +
βTrCP1
Cdc25B^DAA
βTrCP1
Cdc25B^DAA
MKK7
JNK1
β-actin
Cdc25B-IP
WCE
B
WT
D94A
G96A
S101/103A
JNK1
- + - + - + - +
ubiquitylated
Cdc25B^DAA
C
Peptide-conjugated beads
1%input
non-conjugated
non-phospho-25B
phospho-S101-25B
phospho-S101/103-25B
non-phospho-IκBα
phospho-IκBα
short exposure
long exposure
βTrCP1

Fig. 6

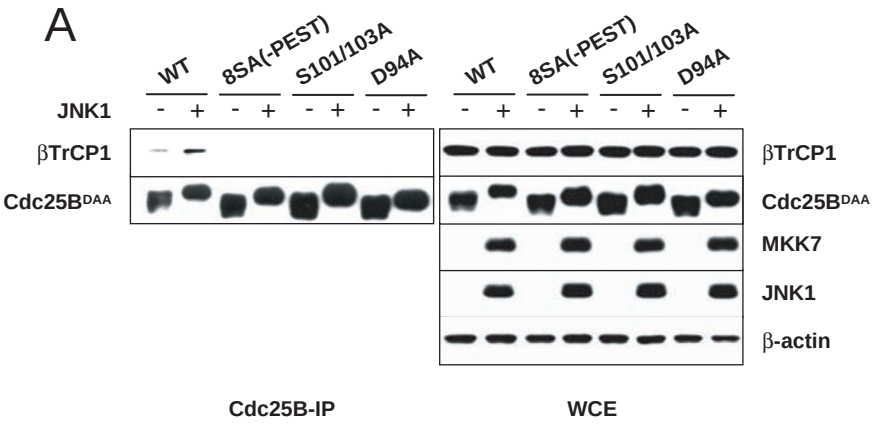
A
WT
8SA(-PEST)
S101/103A
D94A
JNK1
βTrCP1
Cdc25B^DAA
MKK7
β-actin
Cdc25B-IP
WCE

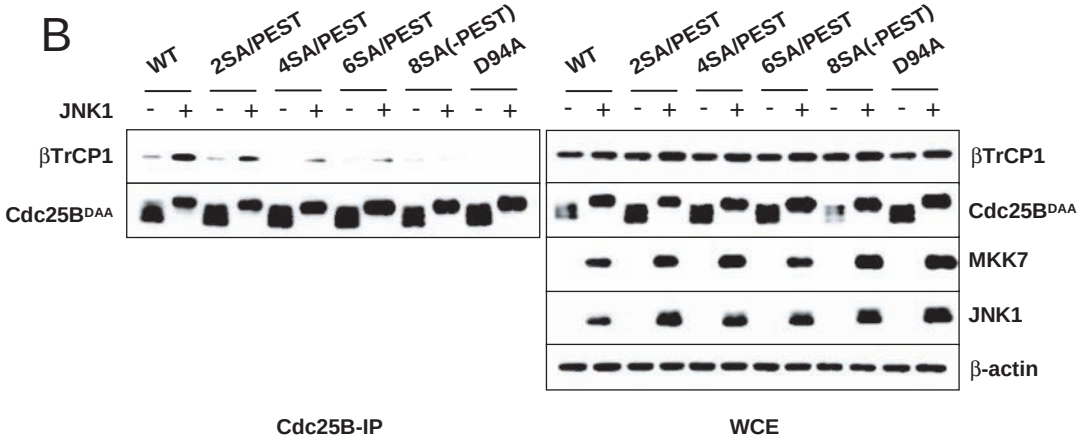
B
WT
2SA/PEST
4SA/PEST
6SA/PEST
8SA(-PEST)
D94A
JNK1
βTrCP1
Cdc25B^DAA
MKK7
β-actin
Cdc25B-IP
WCE

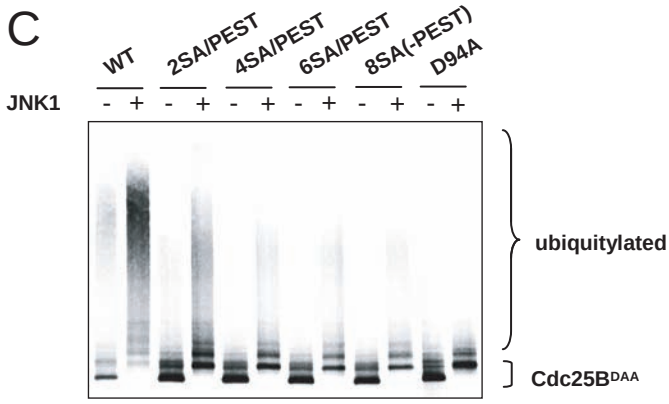
C
WT
2SA/PEST
4SA/PEST
6SA/PEST
8SA(-PEST)
D94A
JNK1
ubiquitylated
Cdc25B^DAA

Fig. 7

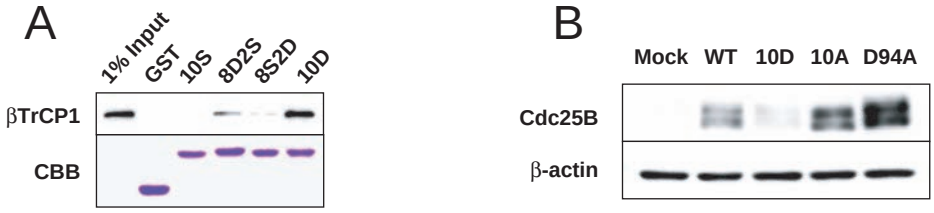
A
1% Input
GST
10S
8D2S
8S2D
10D
βTrCP1
CBB
B
Mock
WT
10D
10A
D94A
Cdc25B
β-actin

Fig. 8

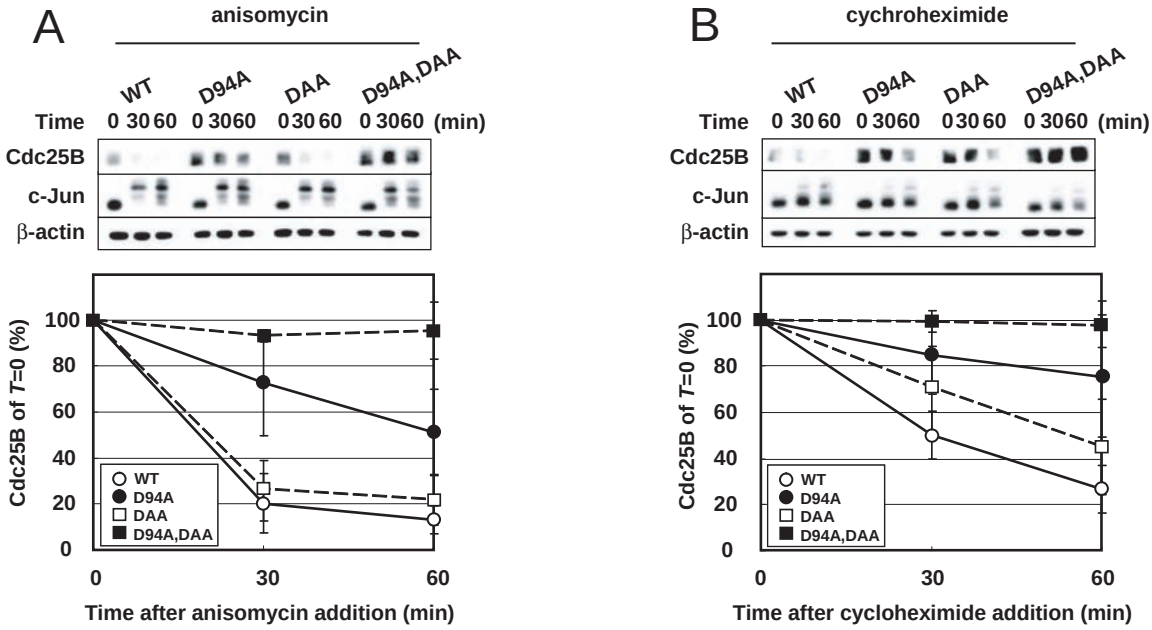
A
anisomycin
WT
D94A
DAA
D94A,DAA
Time
0 30 60 0 30 60 0 30 60 0 30 60 (min)
Cdc25B
c-Jun
β-actin
Cdc25B of T=0 (%)
100
80
60
40
20
0
WT
D94A
DAA
D94A,DAA
0
30
60
Time after anisomycin addition (min)
B
cychroheximide
WT
D94A
DAA
D94A,DAA
Time
0 30 60 0 30 60 0 30 60 0 30 60 (min)
Cdc25B
c-Jun
β-actin
Cdc25B of T=0 (%)
100
80
60
40
20
0
WT
D94A
DAA
D94A,DAA
0
30
60
Time after cycloheximide addition (min)

Supplementary Figure legends

Fig. **S1**. **SCF$^{\beta TrCP}$ ubiquitylates Cdc25B**. (A) ^{35}S-methione-labelled Cdc25B^{DAA} of human B1, human B3, and mouse B1 was incubated with the SCF$^{\beta TrCP}$ complex in the presence or absence of JNK1, and the ubiquitylation was determined as described in the *Materials and Methods*. The ubiquitylation of ^{35}S-methione-labelled Cdc25B1^{DAA} with additional mutations of D94A or S101/103A was also determined. (B) The following FLAG-Cdc25B^{DAA}-based mutants were cotransfected with Myc-βTrCP1 in the presence or absence of JNK1: WT without other mutation; S101A; S103A; S101/103A; or D94A. Then, 24 h later, Cdc25B-bound βTrCP1 was detected by the immunoprecipitation of Cdc25B, followed by immunoblotting (Cdc25B-IP panel). The expression of the indicated proteins is also shown (WCE panel).

Fig. **S2**. **The depletion of βTrCP1/2 with siRNA stabilises Cdc25B**. (A) HeLa cells constitutively expressing FLAG-Cdc25B (HeLa-W40 cells) were transfected with control siRNA (against luciferase (Luci)) or siRNA that targets both βTrCP1 and βTrCP2 (βTrCP). After 24 h, the expression of FLAG-Cdc25B, endogenous Cdc25A, βTrCP1, and β-actin was determined by immunoblotting. (B) HeLa cells were transfected with siRNA against luciferase (Luci) or βTrCP (pan-βTrCP or βTrCP1 + 2).

After 24 h, these cells were further transfected with FLAG-Cdc25B^{DAA} with or without JNK1 and MKK7. After 24 h, the expression of Cdc25B^{DAA} and the indicated proteins was determined by immunoblotting. (C) HeLa-DAA34 cells expressing FLAG-Cdc25B^{DAA} were transfected with siRNA against either Luci or pan-βTrCP and challenged with 50 ng/mL anisomycin. The expression of the indicated proteins was determined by immunoblotting at the indicated time points. Quantitative results for the expression of Cdc25B^{DAA} are shown. The results shown are the average of three independent experiments with the SD.

Fig. S3. Cdc25B S101 and S103 are phosphorylated by JNK or by UV irradiation. (A) The specificity of phospho-specific antibodies was evaluated using *in vitro* phosphorylated Cdc25B. The GST-fused Cdc25B N-terminal fragment (1–175) purified from *E. coli* was phosphorylated by JNK1 and probed with the indicated antibodies. (B) HeLa-W40 cells were irradiated with UV at 20 J/m^2, and cell extracts were prepared at the indicated times. After the immunoprecipitation of Cdc25B with anti-FLAG beads, the phosphorylation status of the indicated amino acids was determined by immunoblotting with each phospho-specific antibody. The expression of the indicated proteins is also shown.

Fig. **S4**. **p38 and JNK are involved in phosphorylation at S101 and S103**.

HeLa-W40 cells were treated with the p38 inhibitor SB202190 (A), p38 inhibitor PD169316 (B), or JNK inhibitor SP600125 (C) at the indicated concentration 1 h before the challenge with 50 ng/mL anisomycin. FLAG-Cdc25B was recovered with anti-FLAG agarose beads, and then the expression and phosphorylation of S101 or S103 was determined by immunoblotting with specific antibodies. The expression of other proteins was also determined. (D) HeLa cells were transfected with the wild-type or kinase-dead form of JNK1 with MKK7. After 24 h, the expression of endogenous Cdc25B was determined by immunoprecipitation followed by immunoblotting. The expression of the indicated proteins is also shown. The transfection efficiency of JNK1 was about 75% (range 70–80%).

Fig. **S5**. **Cdc25B DAG mutations stabilise Cdc25B**. (A) FLAG-Cdc25B of the wild type or D94A, G96A, or S101/103A mutants was cotransfected with or without JNK1. The expression of the indicated proteins was determined 24 h after transfection by immunoblotting. (B) Cdc25B of the wild type, D94A, or S101/103A was cotransfected with or without JNK1. After 24 h, cell extracts were prepared, and Cdc25B was

immunoprecipitated with anti-FLAG beads, followed by the determination of Cdc25B S101/103 phosphorylation by immunoblotting.

Fig. **S6**. **The Cdc25B PEST-like sequence plays an important role in JNK-induced degradation**. (A) FLAG-Cdc25B of the wild-type or PEST-like sequence mutant (all eight serine residues in the PEST-like sequence were mutated to alanine, 8SA [-PEST]), S101/103A, or D94A mutants were transfected into HeLa cells in the presence or absence of JNK1. The expression of the indicated proteins was determined 24 h after transfection. (B) FLAG-Cdc25B of the wild-type or PEST-like sequence mutants in which different numbers of serine residues were mutated to alanine were transfected to HeLa cells with or without JNK1. The expression of the indicated proteins was determined 24 h after transfection. (C) FLAG-Cdc25B mutants with mutations in two serine residues in each ESS unit or in LSS in the PEST-like sequence were transfected with or without JNK1. The expression of the indicated proteins was determined 24 h after transfection. (D) FLAG-Cdc25B of wild type or the E88A, E91A, or D94A mutant was transfected with or without JNK1. The expression of the indicated proteins was determined 24 h after transfection. (E) Cdc25B of the wild type, 8SA (-PEST), S101/103A, or D94A was cotransfected with or without JNK1. After 24 h, cell extracts

were prepared, and Cdc25B was immunoprecipitated with anti-FLAG beads, followed by the determination of Cdc25B S101/103 phosphorylation by immunoblotting.

Fig. **S7**. **DAG is a JNK-dependent βTrCP1 site in Cdc25B and DDG is a JNK-independent site**. FLAG-Cdc25B of the wild type or D94A, DAA, or D94A/DAA mutants was transfected with or without JNK1. After 24 h, the FLAG-Cdc25B proteins were recovered by immunoprecipitation and the βTrCP1 bound to FLAG-Cdc25B or recovered FLAG-Cdc25B was determined by immunoblotting (Cdc25B-IP). The expression of the indicated proteins 24 h after transfection is also shown (WCE).

Fig. S1

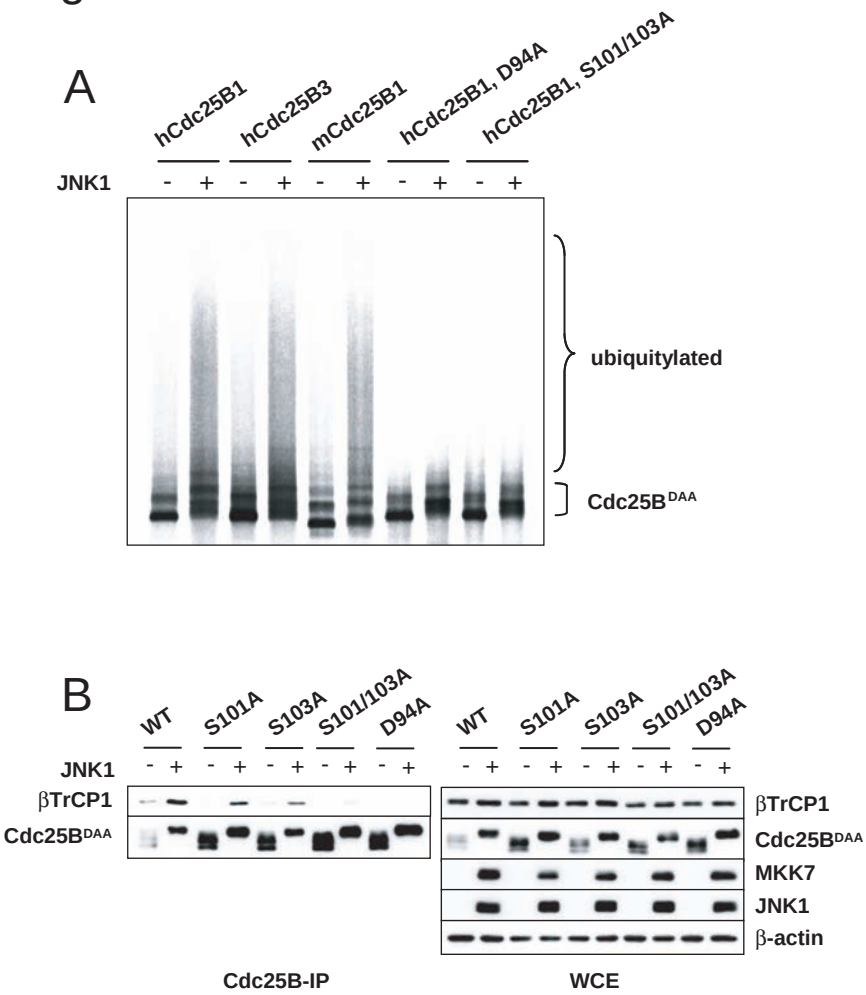
A
hCdc25B1
hCdc25B3
mCdc25B1
hCdc25B1, D94A
hCdc25B1, S101/103A
JNK1
- + - + - + - + - +
ubiquitylated
Cdc25B DAA
B
WT
S101A
S103A
S101/103A
D94A
JNK1
βTrCP1
Cdc25B DAA
MKK7
JNK1
β-actin
Cdc25B-IP
WCE

Fig. S2

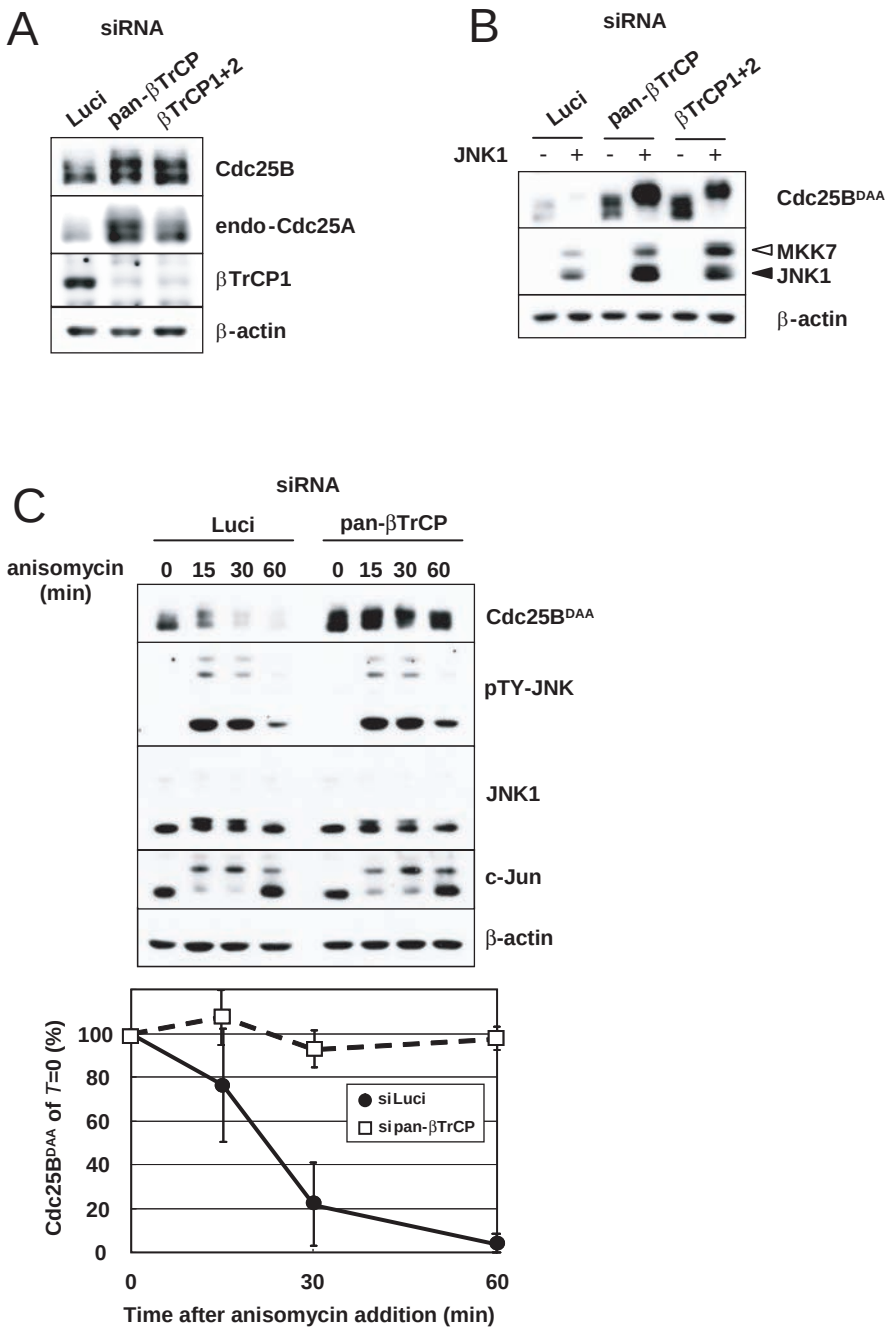
A
siRNA
Luci
pan-βTrCP
βTrCP1+2
Cdc25B
endo-Cdc25A
βTrCP1
β-actin
B
siRNA
Luci
pan-βTrCP
βTrCP1+2
JNK1
- + - + - +
Cdc25BDAA
MKK7
JNK1
β-actin
C
siRNA
Luci
pan-βTrCP
anisomycin (min)
0 15 30 60 0 15 30 60
Cdc25BDAA
pTY-JNK
JNK1
c-Jun
β-actin
Cdc25BDAA of T=0 (%)
100
80
60
40
20
0
siLuci
sipan-βTrCP
0
30
60
Time after anisomycin addition (min)

Fig. S3

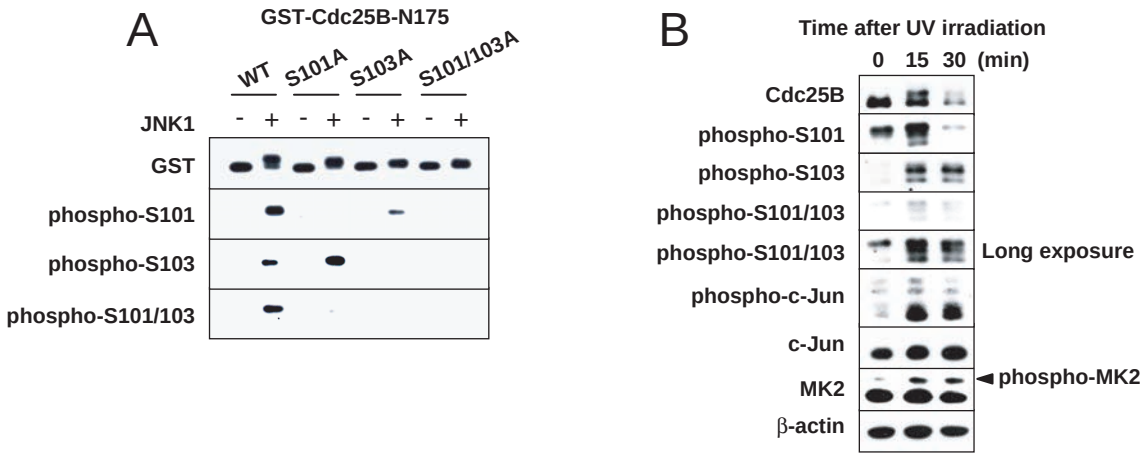
A
GST-Cdc25B-N175
WT
S101A
S103A
S101/103A
JNK1
- + - + - + - +
GST
phospho-S101
phospho-S103
phospho-S101/103
B
Time after UV irradiation
0 15 30 (min)
Cdc25B
phospho-S101
phospho-S103
phospho-S101/103
phospho-S101/103
Long exposure
phospho-c-Jun
c-Jun
MK2
phospho-MK2
β-actin

Fig. S4

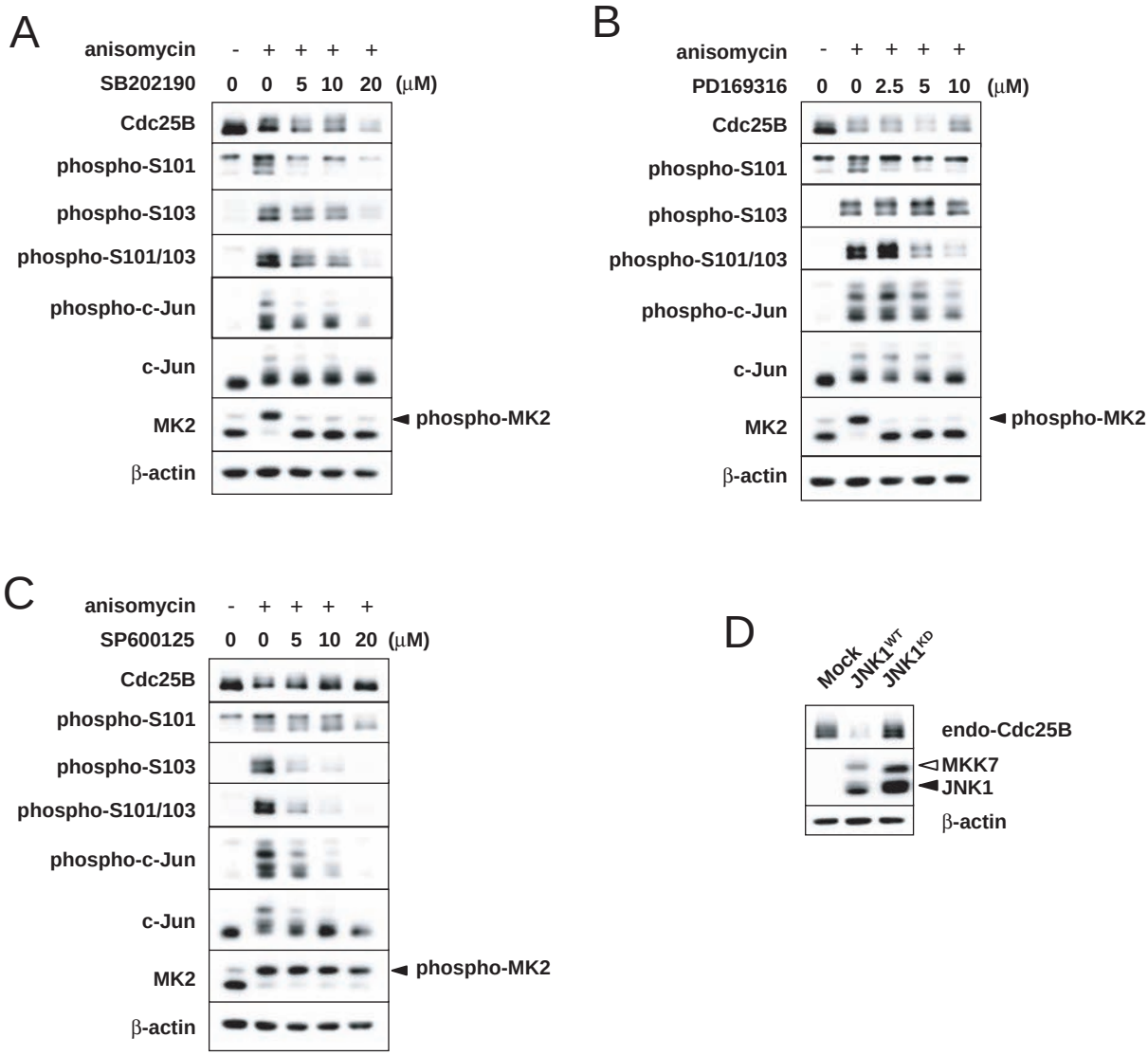
A
anisomycin - + + + +
SB202190 0 0 5 10 20 (μM)
Cdc25B
phospho-S101
phospho-S103
phospho-S101/103
phospho-c-Jun
c-Jun
MK2
β-actin
phospho-MK2
B
anisomycin - + + + +
PD169316 0 0 2.5 5 10 (μM)
Cdc25B
phospho-S101
phospho-S103
phospho-S101/103
phospho-c-Jun
c-Jun
MK2
β-actin
phospho-MK2
C
anisomycin - + + + +
SP600125 0 0 5 10 20 (μM)
Cdc25B
phospho-S101
phospho-S103
phospho-S101/103
phospho-c-Jun
c-Jun
MK2
β-actin
phospho-MK2
D
Mock
JNK1WT
JNK1KD
endo-Cdc25B
MKK7
JNK1
β-actin

Fig. S5

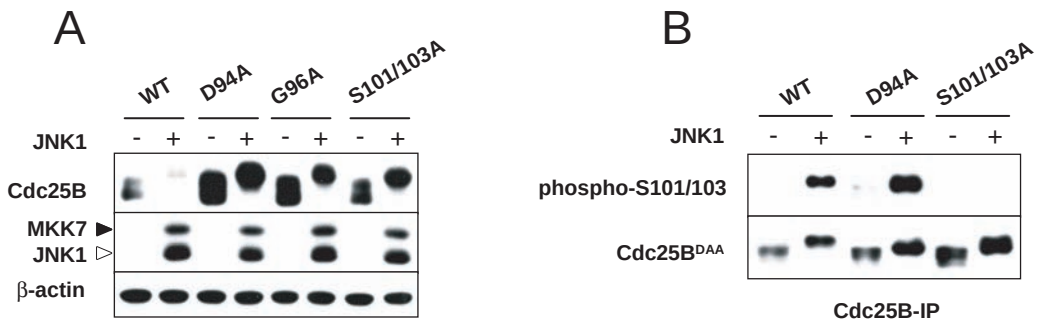
A
WT
D94A
G96A
S101/103A
JNK1
- + - + - + - +
Cdc25B
MKK7
JNK1
β-actin
B
WT
D94A
S101/103A
JNK1
- + - + - +
phospho-S101/103
Cdc25B^DAA
Cdc25B-IP

Fig. S6

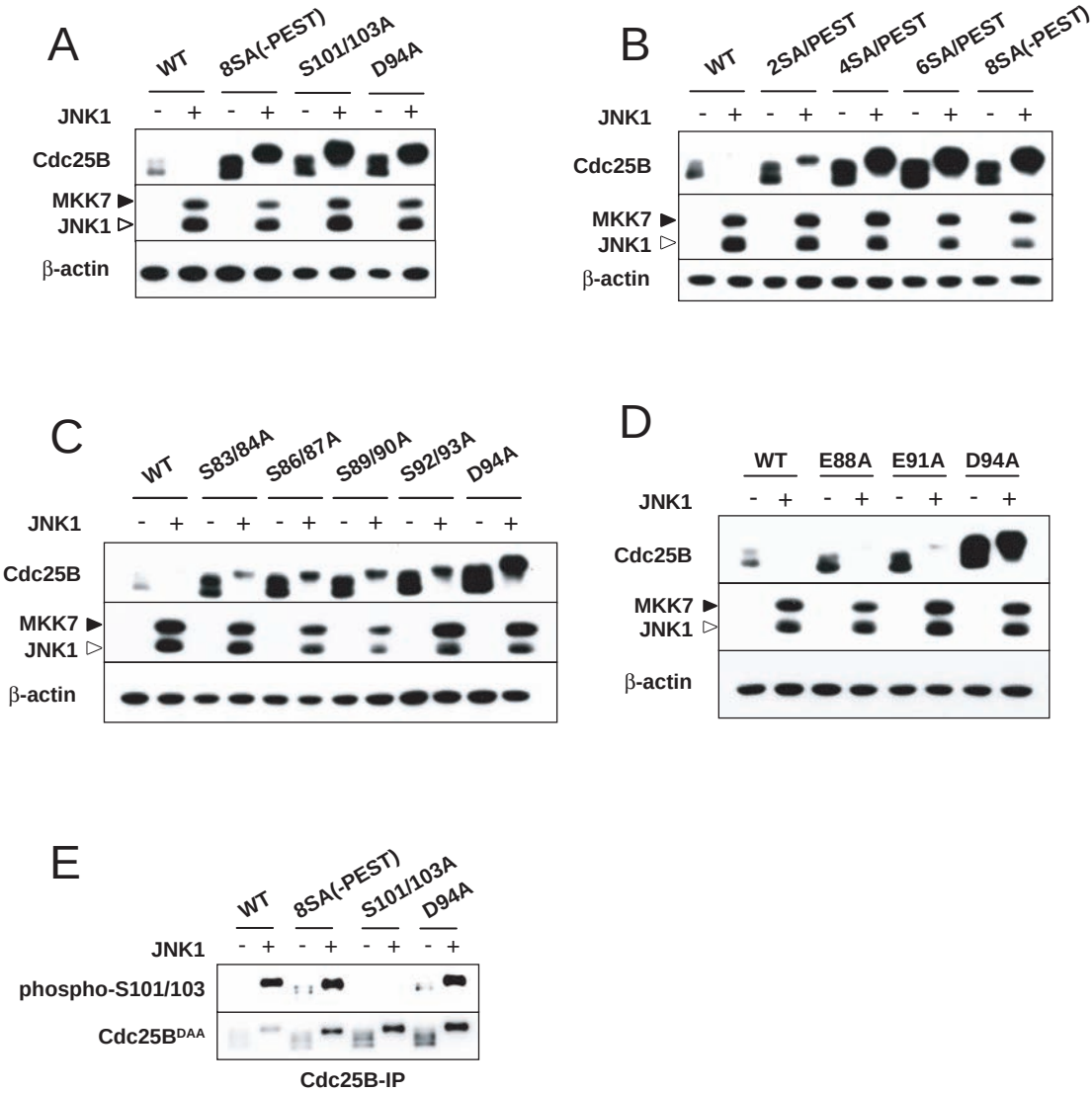
A
WT
8SA(-PEST)
S101/103A
D94A
JNK1
- + - + - + - +
Cdc25B
MKK7 ▶
JNK1 ▷
β-actin
B
WT
2SA/PEST
4SA/PEST
6SA/PEST
8SA(-PEST)
JNK1
- + - + - + - + - +
Cdc25B
MKK7 ▶
JNK1 ▷
β-actin
C
WT
S83/84A
S86/87A
S89/90A
S92/93A
D94A
JNK1
- + - + - + - + - + - +
Cdc25B
MKK7 ▶
JNK1 ▷
β-actin
D
WT
E88A
E91A
D94A
JNK1
- + - + - + - +
Cdc25B
MKK7 ▶
JNK1 ▷
β-actin
E
WT
8SA(-PEST)
S101/103A
D94A
JNK1
- + - + - + - +
phospho-S101/103
Cdc25B^DAA
Cdc25B-IP

Fig. S7

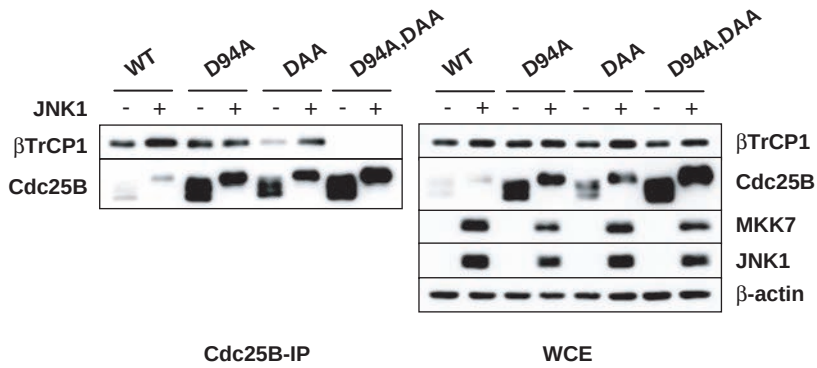
WT
D94A
DAA
D94A,DAA
WT
D94A
DAA
D94A,DAA
JNK1
- + - + - + - +
- + - + - + - +
βTrCP1
Cdc25B
βTrCP1
Cdc25B
MKK7
JNK1
β-actin
Cdc25B-IP
WCE